U.S.NRC
UNITED STATES NUCLEAR REGULATORY COMMISSION
Protecting People and the Environment

Importance of Microstructural Analysis and Modeling in Understanding the Degradation of Materials

Appajosula Rao
Corrosion and Metallurgy Branch
Division of Engineering
Office of Nuclear Regulatory Research (RES)

NRC Research Seminar, USNRC Sept. 12th 2017

Disclaimer

This presentation [report] was prepared as an account of work sponsored by an agency of the U.S. Government. Neither the U.S. Government nor any agency thereof, nor any of their employees, makes any warranty, expressed or implied, or assumes any legal liability or responsibility for any third party's use, or the results of such use, of any information, apparatus, product, or process disclosed in this presentation [report], or represents that its use by such third party would not infringe privately owned rights. The views expressed in this paper are not necessarily those of the U.S. Nuclear Regulatory Commission.

U.S.NRC
UNITED STATES NUCLEAR REGULATORY COMMISSION
Protecting People and the Environment

Outline

- Background
  - Regulatory Research on Reactor Pressure Vessel (RPV) Internals
  - Materials science based logic for radiation induced material degradation
  - Materials science based logic for modeling general material degradation
- Materials investigated and the testing protocol
- Recent NRC research on RPV internals
  - Effect of radiation on mechanical properties
  - Transmission electron microscopy (TEM) analysis of the microstructure of irradiated stainless steels and cast stainless steels (CASS)
- Atom probe tomography (APT)
- High energy x-ray diffraction data processing and data analysis.
- Modeling effort
- Summary
- Acknowledgement

Background

Regulatory Research on RPV Internals (RVIs)

- Regulatory framework for RVIs
  - ➢ RES supports the NRC regulatory decision making authority by providing required technical basis
- NRC-sponsored research on RVIs
  - – Irradiation-assisted degradation of stainless steel plate and weld materials
  - – Embrittlement of CASS
- Regulatory perspective
  - – High impact on license renewal and inspection decision, and aging management strategy
  - – Subsequent license renewal guidance documents (NUREG-2191 and NUREG-2192)

Background (cont.) Materials Science Logic

- For a Given System → It is Important to Know

→ Why
→ When
→ Where
→ How

→ What ?

Ex.: What → Material Degradation

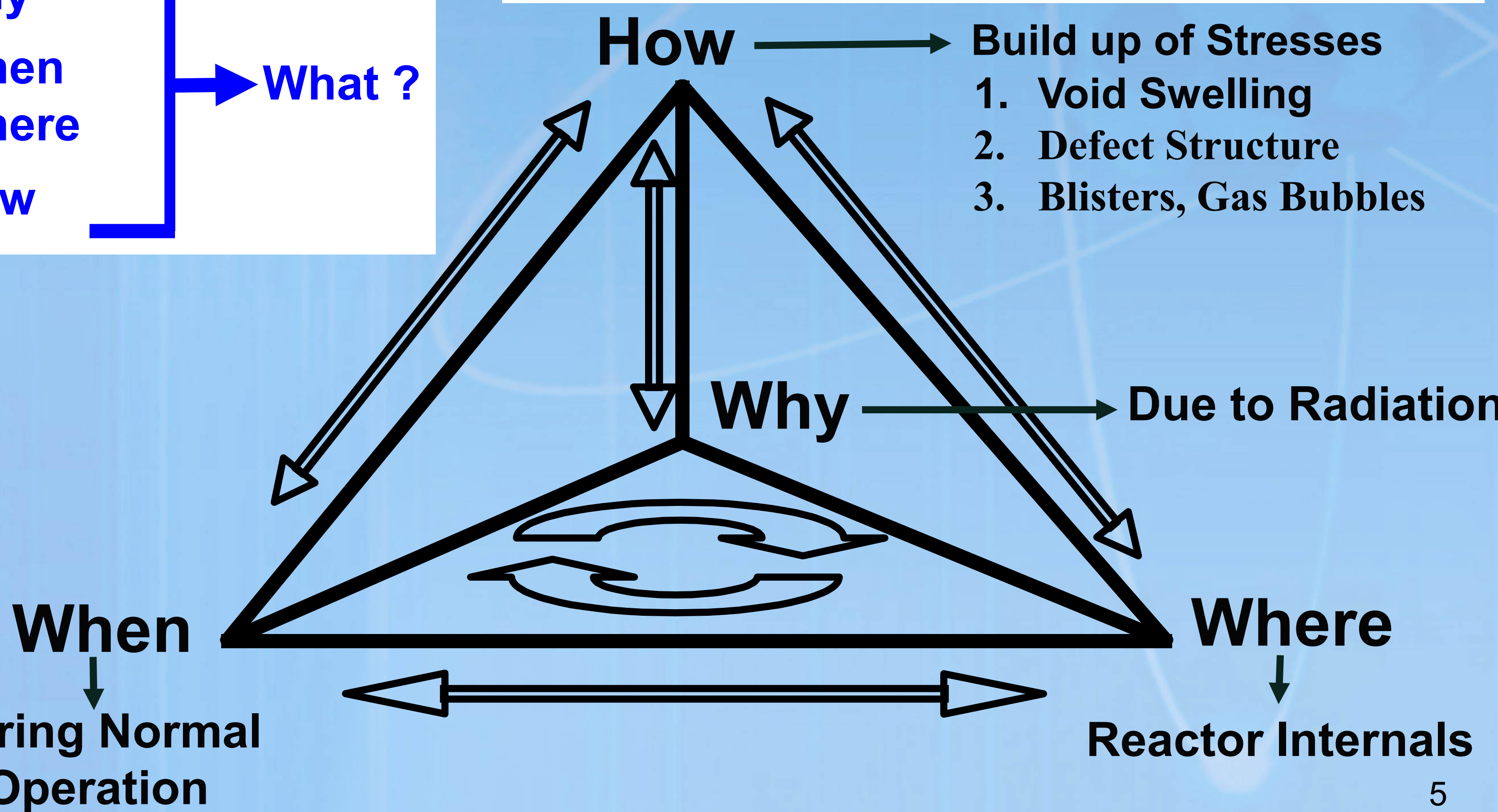

Materials science based logic for modeling general material degradation

U.S.NRC
UNITED STATES NUCLEAR REGULATORY COMMISSION
Protecting People and the Environment

Model → **Based on the changes of stress / strain in materials using**

Analytical modeling
Finite element analysis techniques

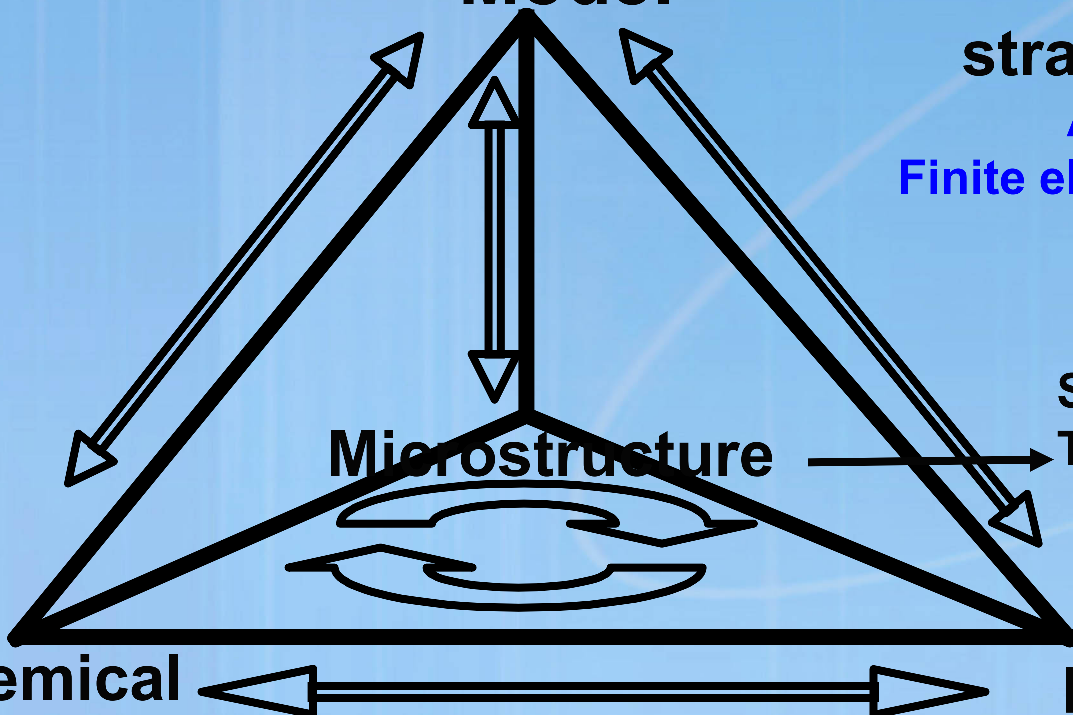

Microstructure → SEM – Topological Changes
TEM – Microstructural Changes

Chemical changes ↔ **Changes in the physical structure**

Chemical changes ↓

Changes in the chemical composition
using Atom Probe Tomography (APT)

Changes in the physical structure ↓

On the Surface or Within the Structure

Mechanical properties
Hardness using Nano indentation
Structure using X-ray diffraction (XRD)

Materials investigated and the testing protocol

- **Materials Investigated:**
  - Stainless Steels (304 L, 304L SA, 304 CW, 316 CW)
  - Cast Stainless Steels (CF-3, CF-8 and CF-8 M grade)
- **Neutron irradiation condition**
  - Stainless Steels (1- 40 dpa) ** using either LWR or fast reactor neutron irradiation*
  - Cast Stainless Steels (0.089 to 3 dpa) *under LWR irradiation condition*
- **Test environment**
  - LWR condition
- **Tests conducted on these steel materials**
  - Crack growth rate (CGR)
  - Fracture toughness (FT)
  - Microstructural Examination - Using
    - Scanning electron microscope (SEM)
    - Transmission electron microscope (TEM)
    - Atom probe tomography (APT)
    - High energy X-ray diffraction using Synchrotron Radiation Facility

U.S.NRC
UNITED STATES NUCLEAR REGULATORY COMMISSION
Protecting People and the Environment

Recent NRC Research on RPV Internals

- Effect of radiation on mechanical properties

Irradiation hardening

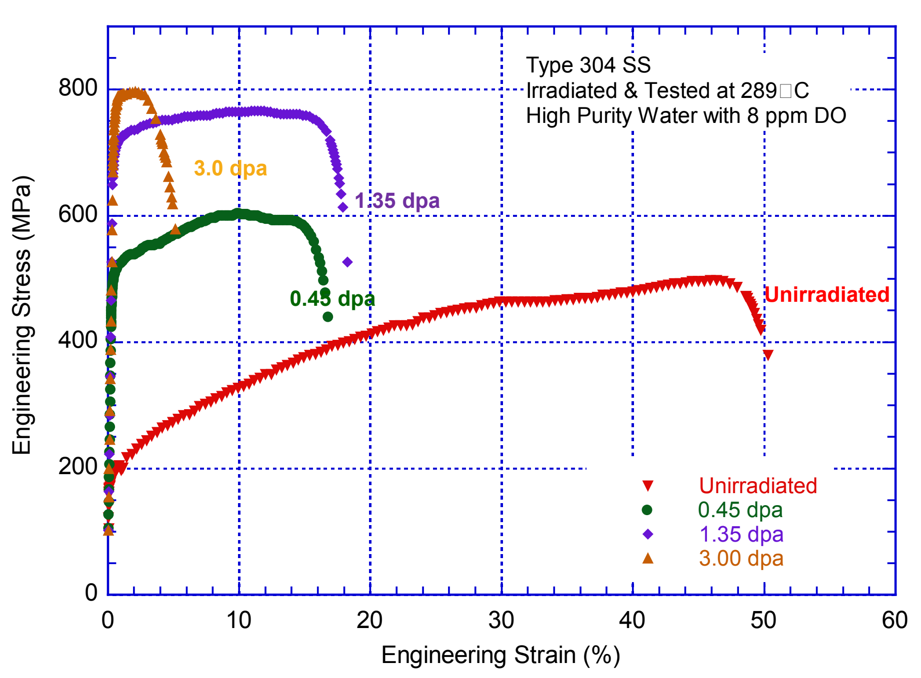

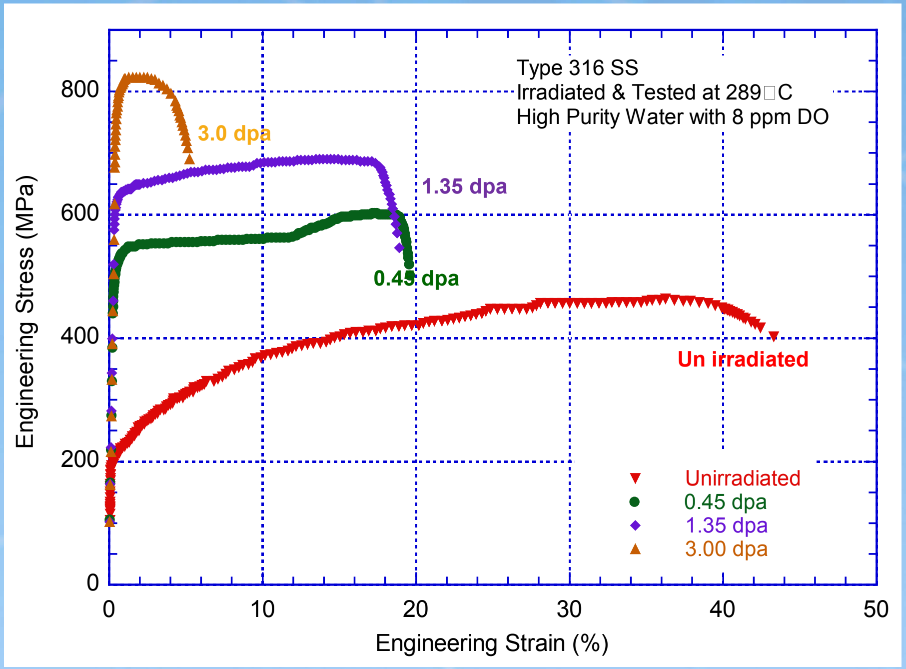

Ref: Y. Chen et al., NUREG/CR – 7128(2012)

- **Defect structure & precipitates act as obstacles to dislocation motion that lead to matrix strengthening - increase in yield strength & decrease in ductility**
- **In general, cavities (voids) are strong barriers, large faulted dislocation loops are intermediate barriers, & small loops & bubbles are weak barriers**

Increase in yield stress - type 316 SS

Irradiation temperature 90-427°C, test temperature 100-427°C

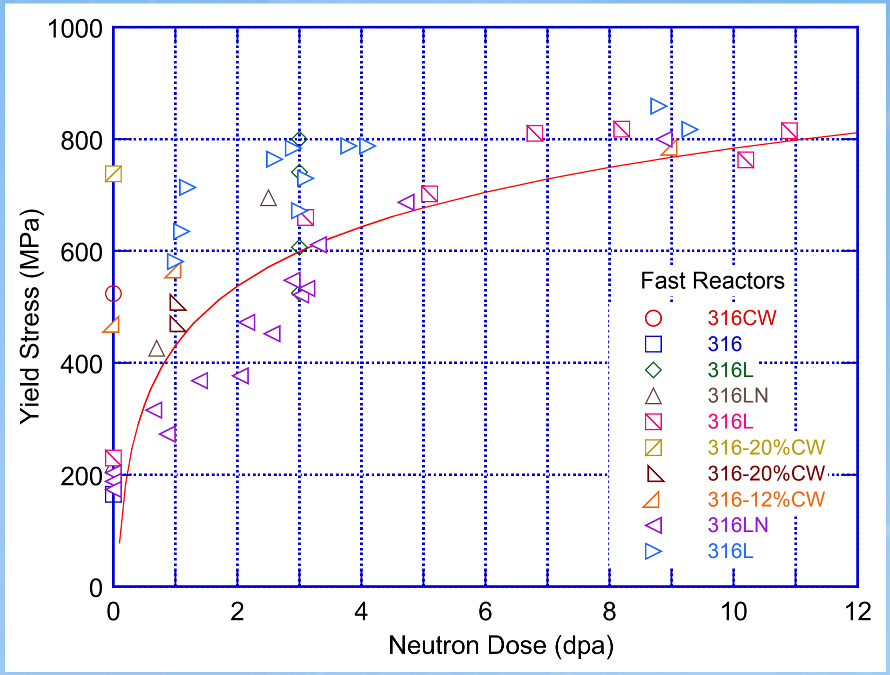

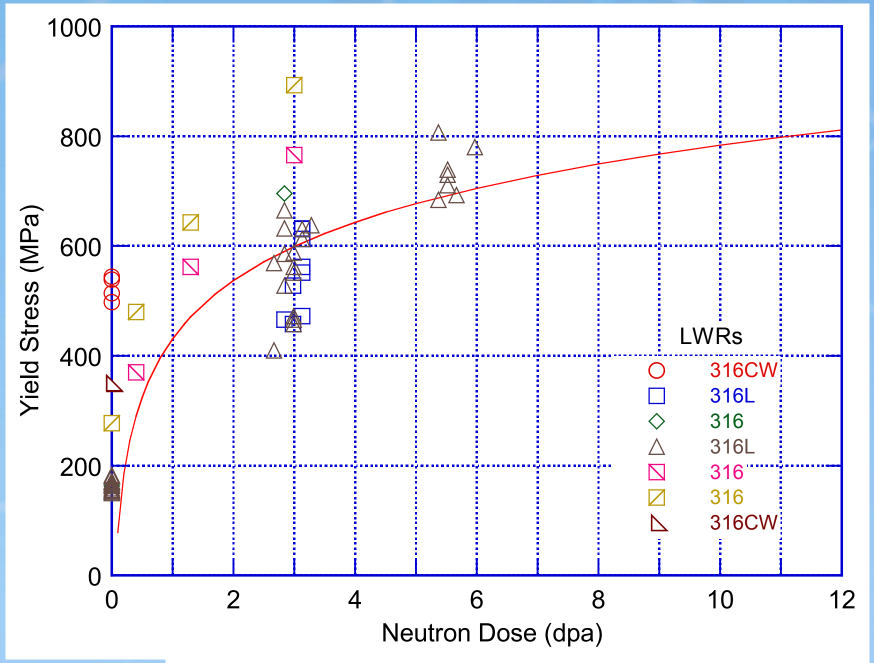

Ref: Y, Chen et al., NUREG/CR – 7128(2012)

- **YS of SA SS increases from 180-250 to ≈800 MPa at 3-5 dpa**
- **YS of cold worked SS increases from 500-700 to ≈1000 MPa at 3-5 dpa**
- **Effect of fast reactor and LWR irradiation on the YS of materials is the same**

Micro-chemical changes at the grain boundary of steels versus neutron irradiation

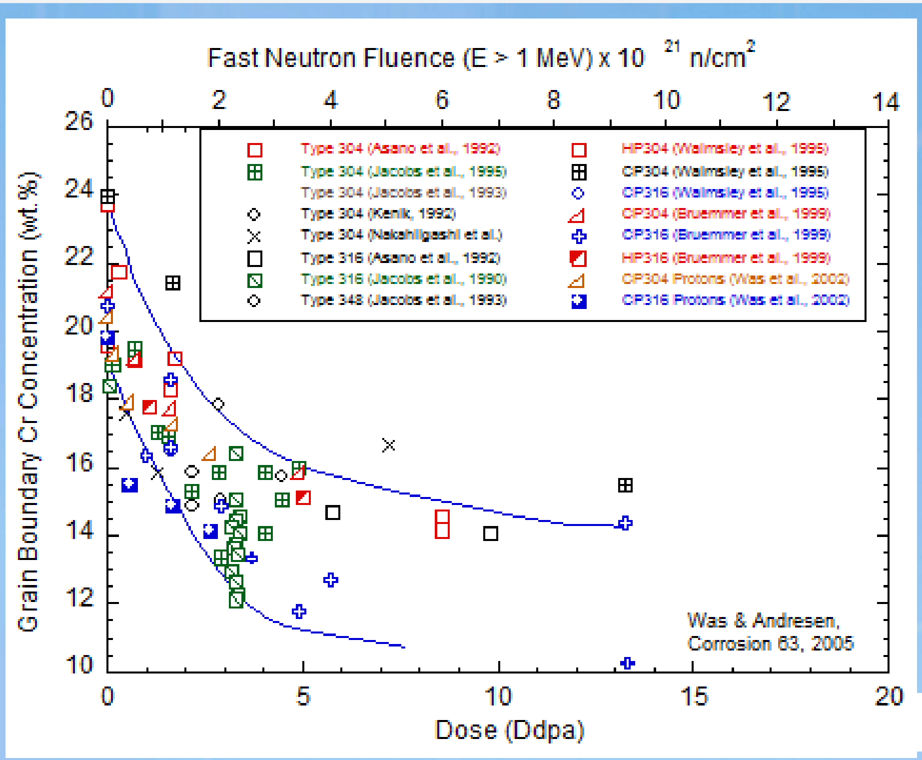

Ref: Chopra, NUREG/CR – 7027(2010)

- Radiation induced segregation (RIS) results in grain boundary (GB) depletion of Cr, Mn, Mo & enrichment of Ni, Si, P, C, B
- Segregation depends strongly on irradiation temperature, dose, & dose rate
- In LWRs, RIS increases with neutron dose, peaks at intermediate temp, & increases at lower dose rates
- At 300°C, saturates at ≈5 dpa

UNITED STATES NUCLEAR REGULATORY COMMISSION
Protecting People and the Environment

Dose Dependence of grain boundary Cr, Ni & Si contents for stainless steels irradiated in LWRs and fast reactors

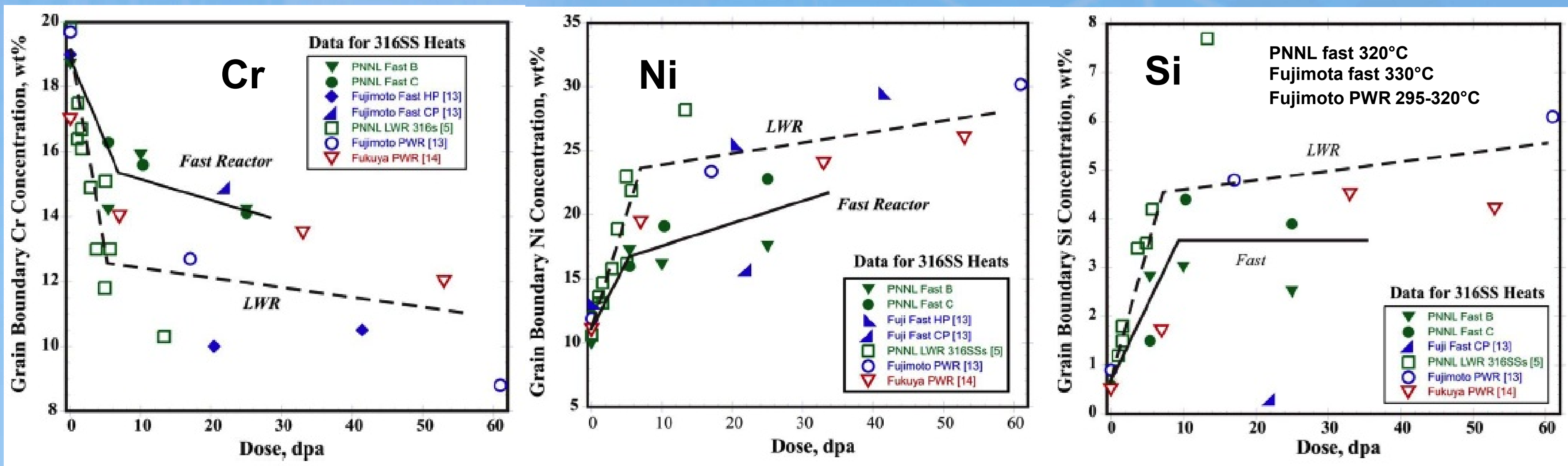

Ref: Data from Edwards et al., 13th Intl. Conf. Env. Degrad., P0139, 2007

- RIS results in GB depletion of Cr and the enrichment of Ni, Si.
- Stronger RIS in LWRs than BOR-60 (except data from *Fujimoto fast HP*), particularly above 5 dpa
- Irradiation temperature comparable, differences most likely due to dose rate

Slow Strain Rate Test (SSRT) Results

Type 304 and 304L SSs
Irradiation BOR-60 fast reactor

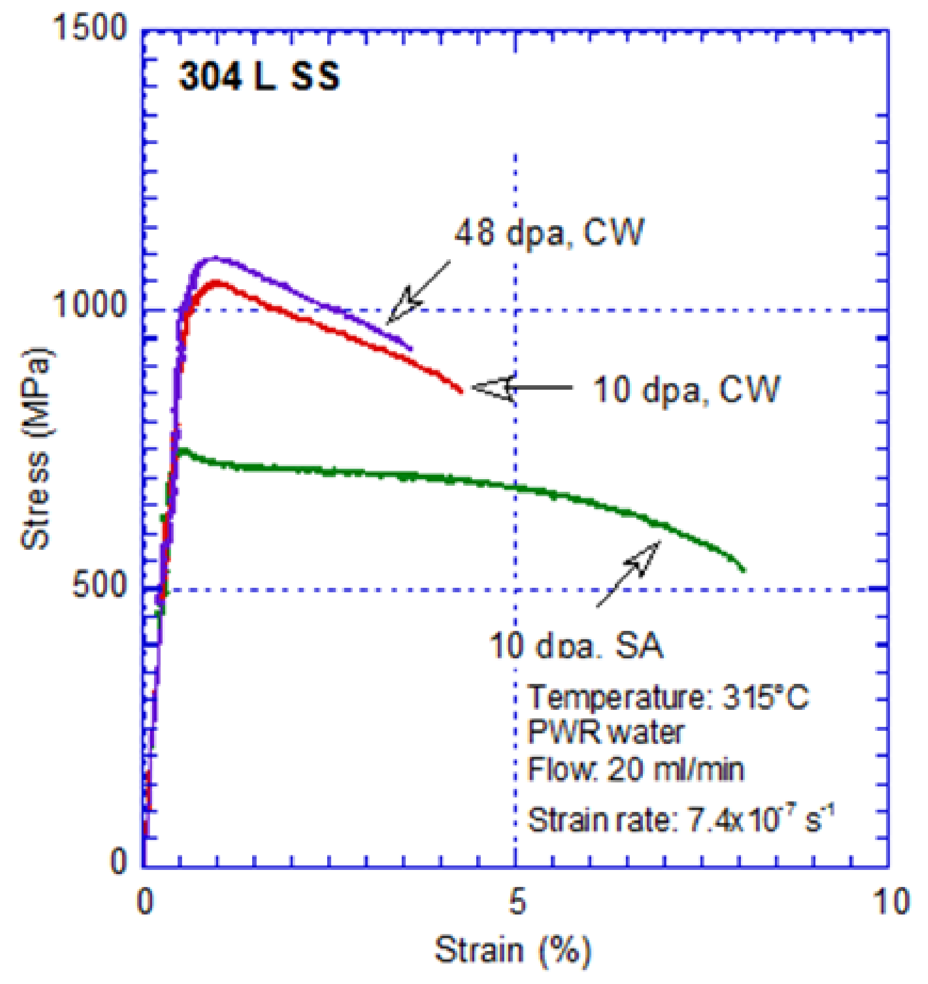

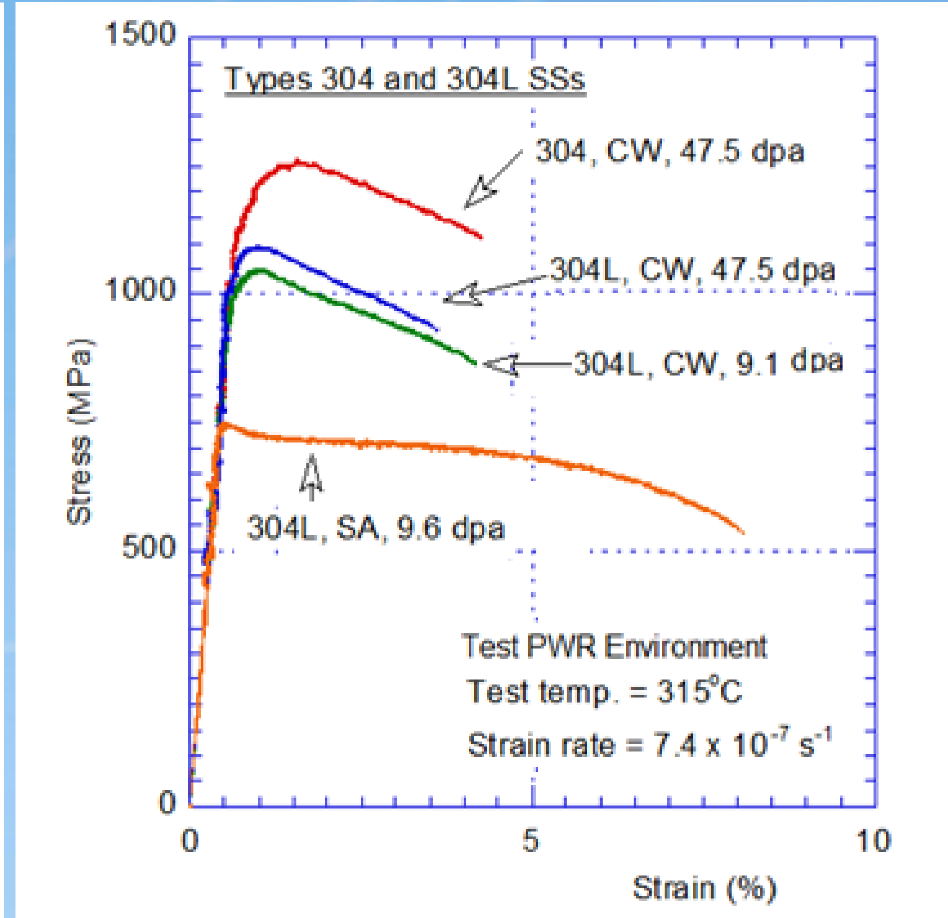

Ref: Y. Chen et al., NUREG/CR – 7018(2010) and 6965 (2008)

- CW samples exhibit much higher yield stress and less elongation.

U.S.NRC
UNITED STATES NUCLEAR REGULATORY COMMISSION
Protecting People and the Environment

Microstructure of SA and CW type 304L SS

304L SA, 10 dpa

Large dimples

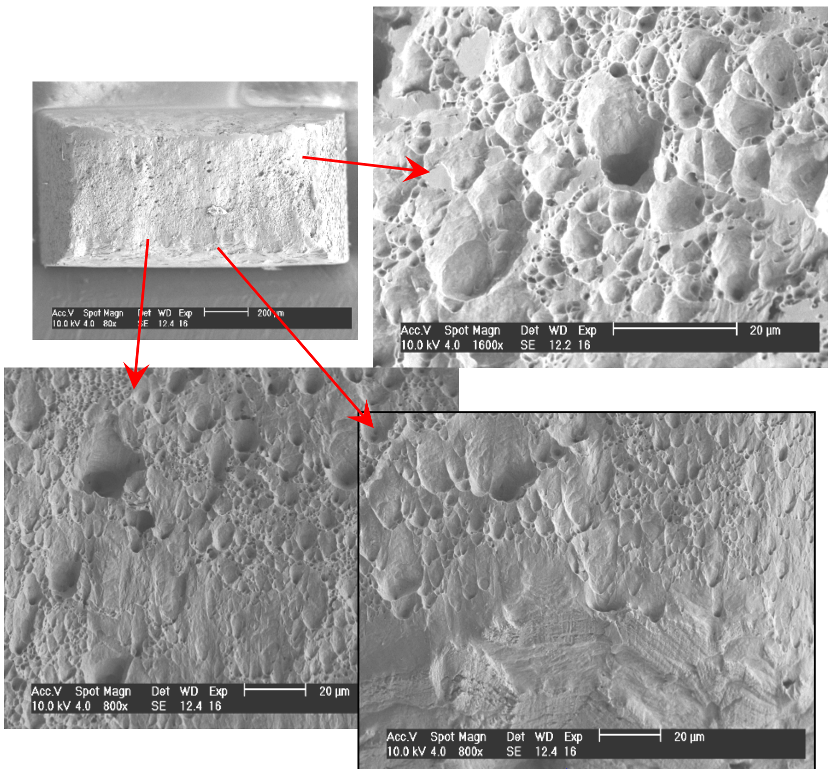

304L CW, 10 dpa

Small dimples with some brittle areas

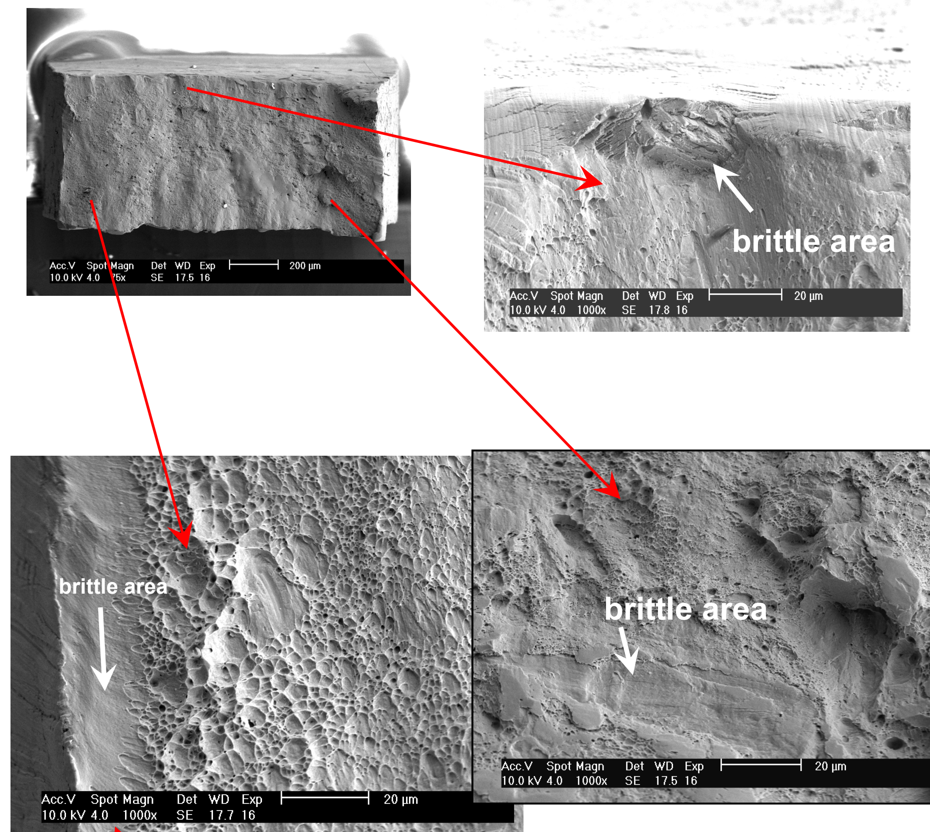

SA samples possess fully ductile features while brittle features can be seen in CW samples.

Ref: Y, Chen et al., NUREG/CR – 7018(2010) and 6965 (2008)

U.S.NRC
UNITED STATES NUCLEAR REGULATORY COMMISSION
Protecting People and the Environment

Microstructure of irradiated type 304L CW SS

10-dpa

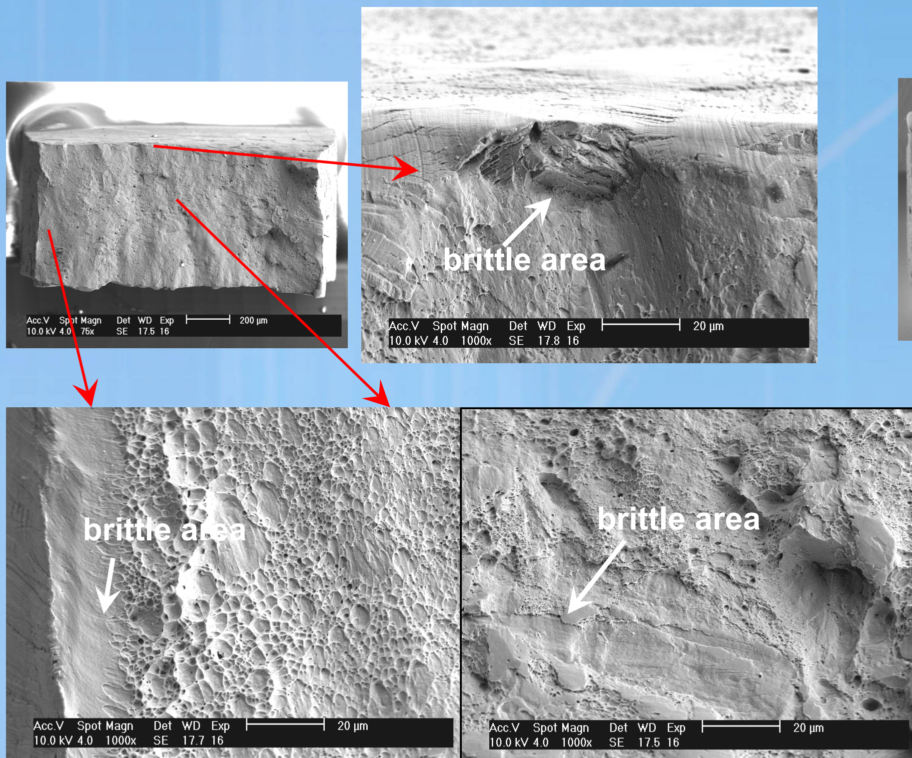

48-dpa

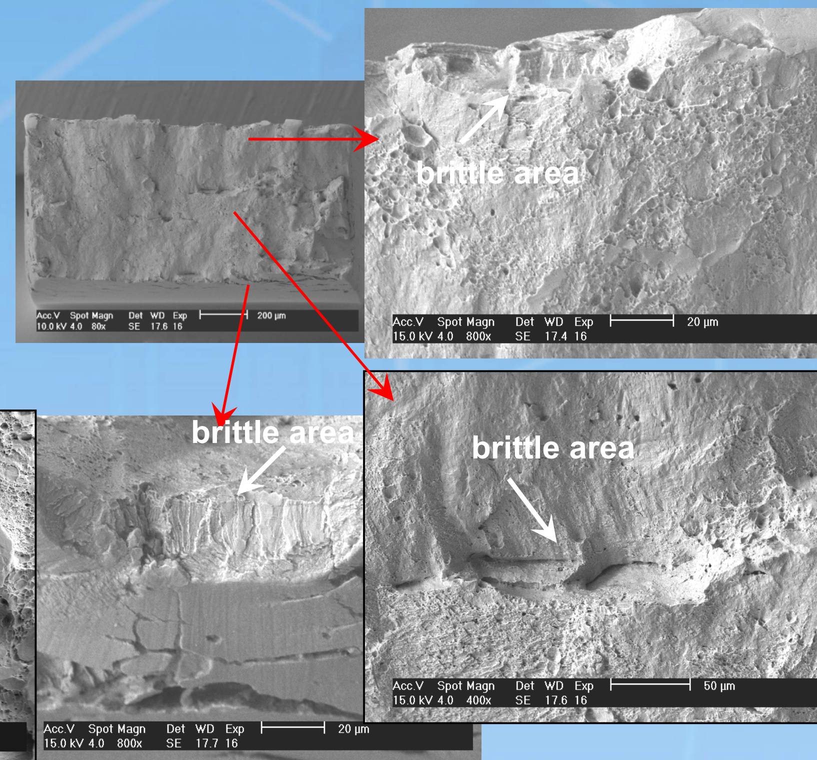

Small dimples with some brittle areas

More brittle areas in higher dose sample and cleavage on sample surface.

Ref: Y, Chen et al., NUREG/CR – 7018(2010) and 6965 (2008)

Yield stress - dose effects SA versus CW

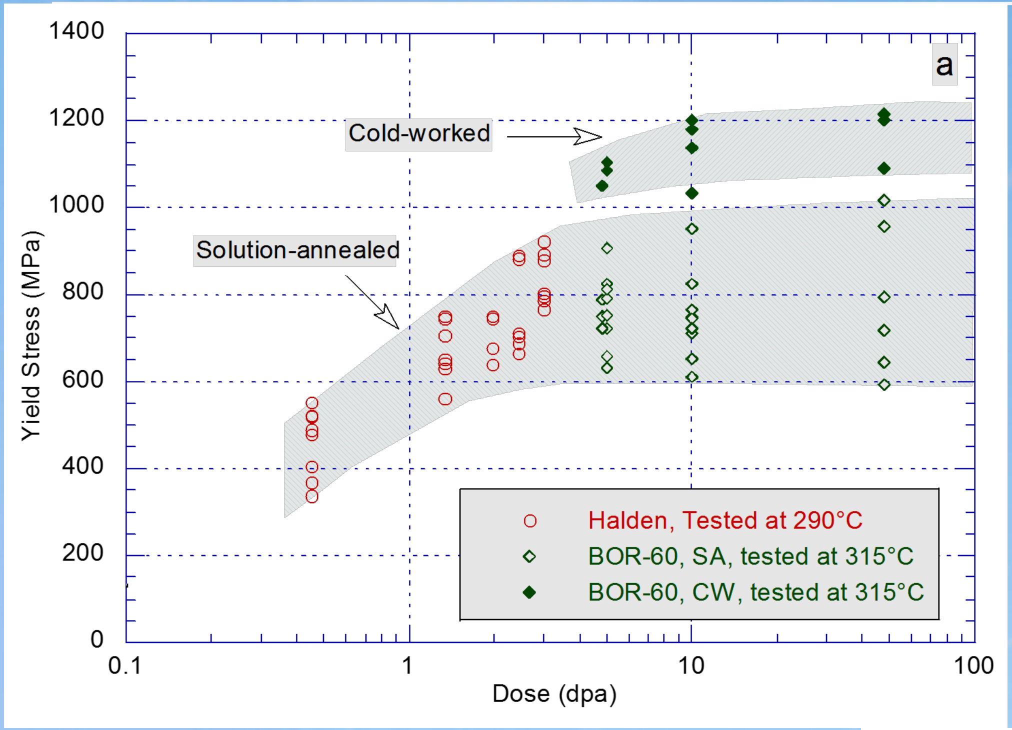

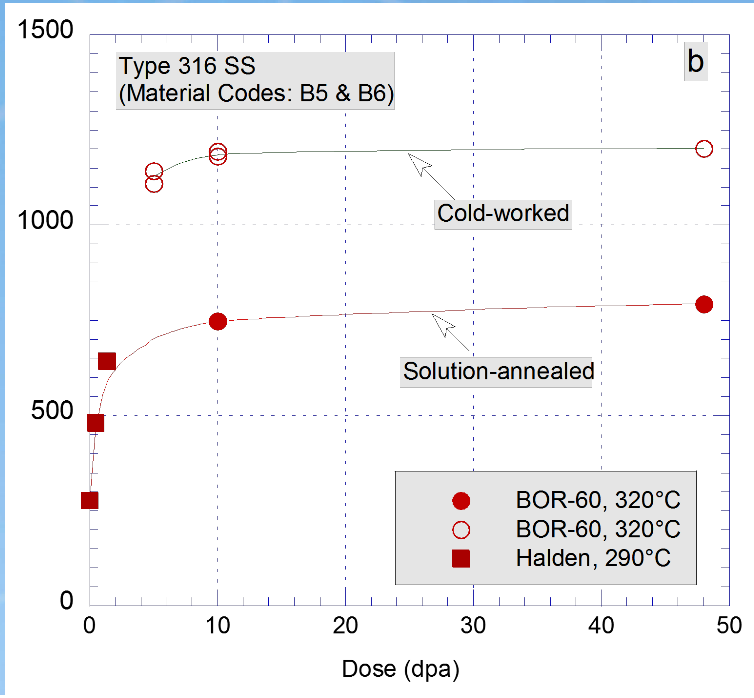

Ref: Y, Chen et al., NUREG/CR – 7018(2010) and 6965 (2008)

- The increase of yield stress by CW is not affected by irradiation beyond 10 dpa.
- The yield stress differences between SA and CW materials are consistent between 10 to 48 dpa.
- The yield stress seems to saturate at 5-10 dpa.

SSRT Tests - Effect of Sulfur Content

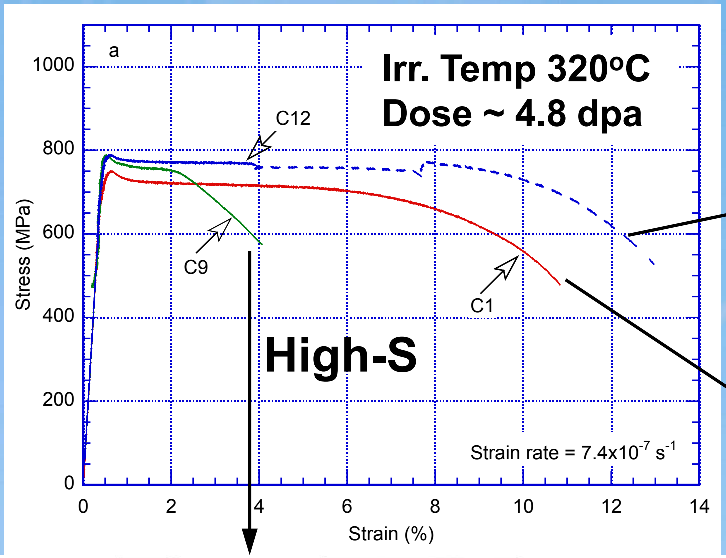

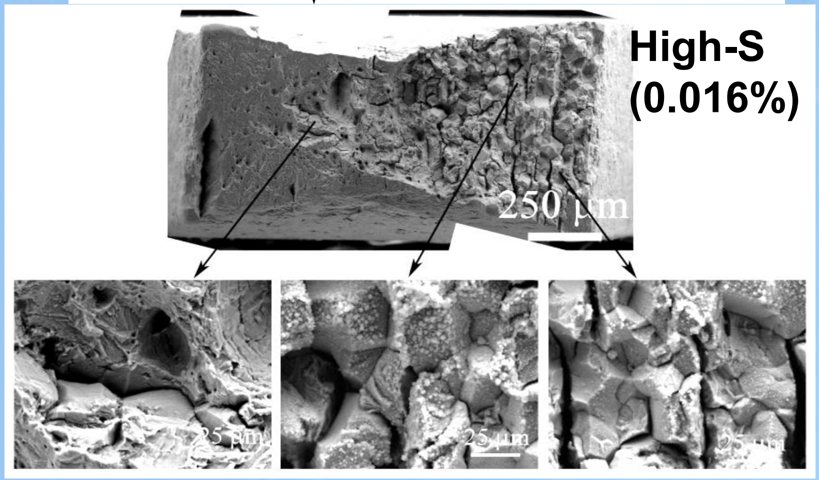

Low-S

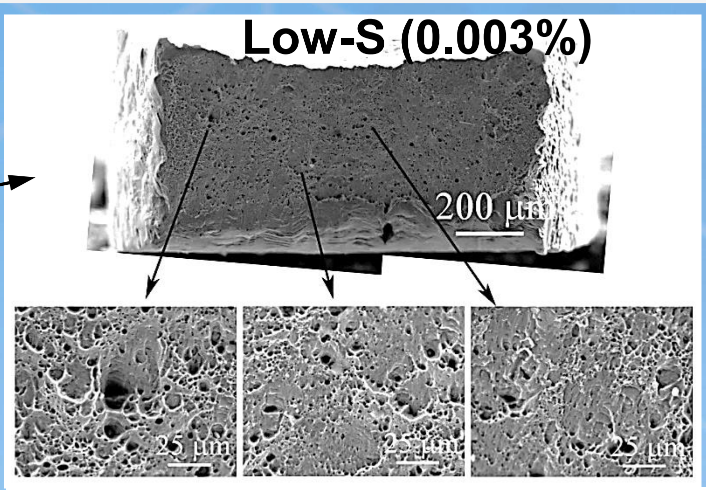

Low-S

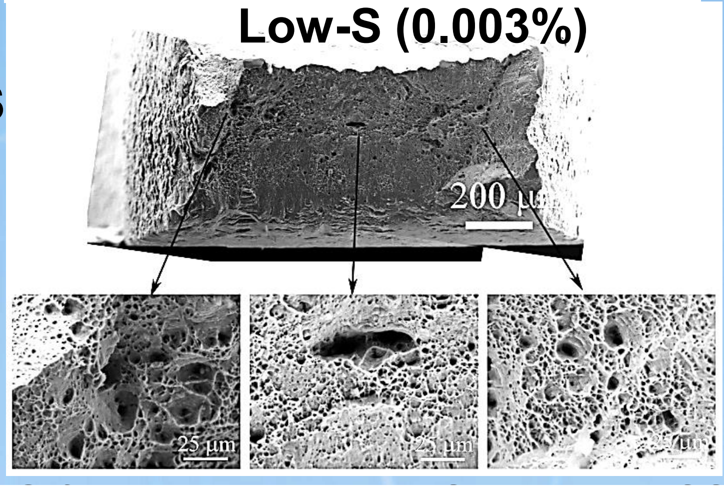

Ref: Y, Chen et al., NUREG/CR – 7018(2010) and 6965 (2008)

Inter-granular (IG) cracking is severe in the high-S Type 304 SS

HP Type 304L SS SA with high - O (0.008%) and low-O (0.0047%)

U.S.NRC
UNITED STATES NUCLEAR REGULATORY COMMISSION
Protecting People and the Environment

Test DO Environment

High-O, RA ~ 60%

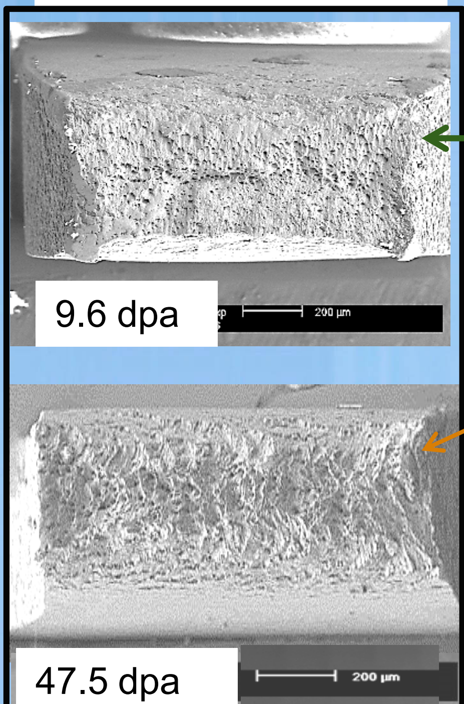

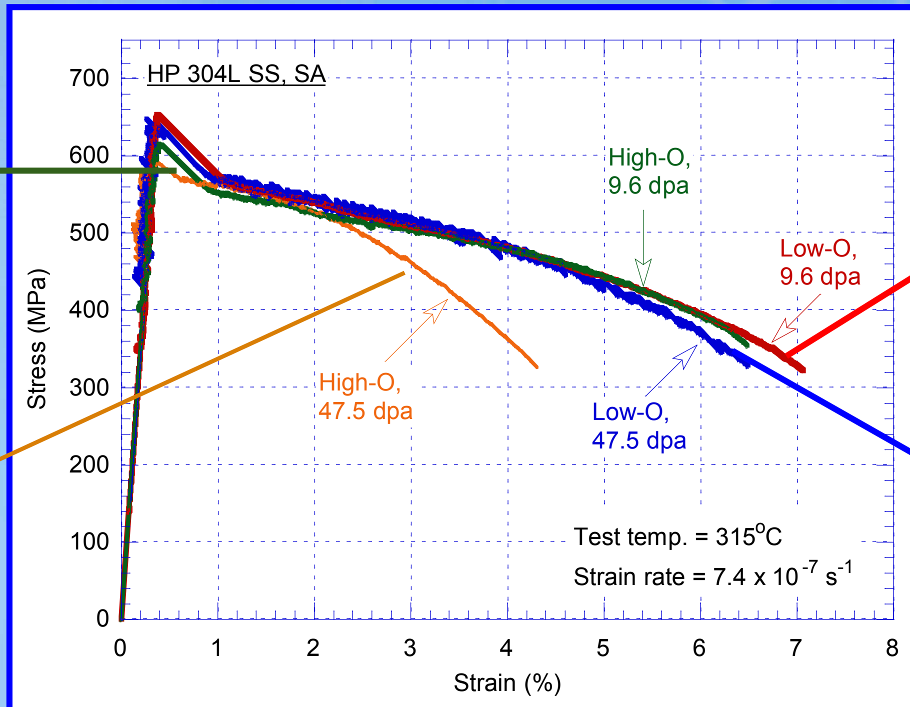

Low-O, RA ~ 80%

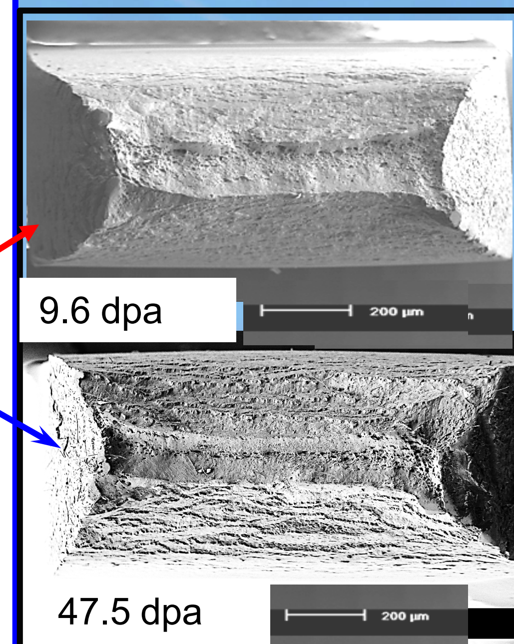

Ref: Y, Chen et al., NUREG/CR – 7018(2010) and 6965 (2008)

- **A load drop beyond yield is observed for all HP 304L samples, regardless of their oxygen content.**
- **The low-O specimens are more ductile than the high-O specimens.**
- **No IG cracking was observed in low-O specimens .**

Note: RA - reduction in area of cross-section of a sample

HP 304L SS – 48 dpa, low-O vs. high-O

RA≈76%, dimples   48 dpa, <u>Low-O</u>

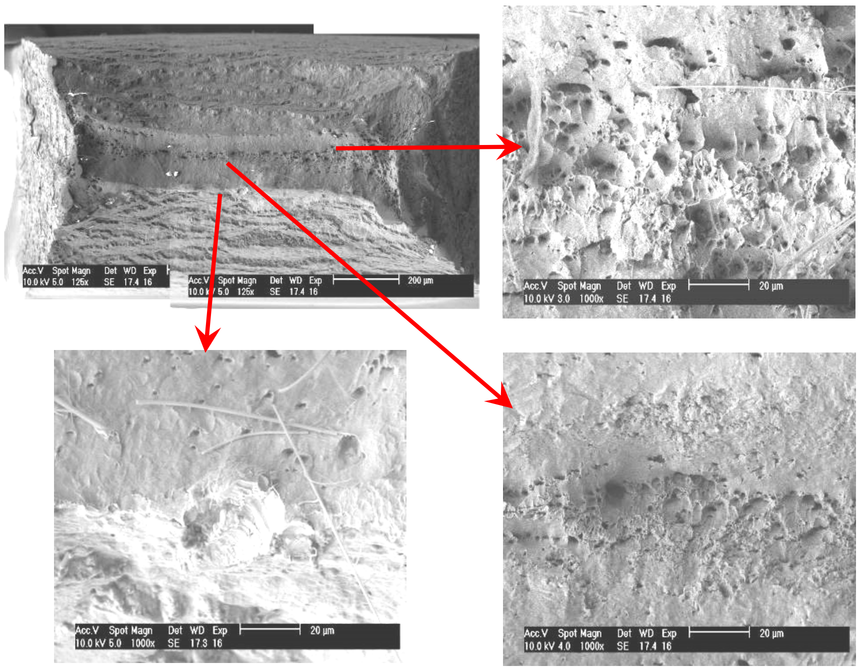

RA≈58%, dimples   48 dpa, <u>High-O</u>

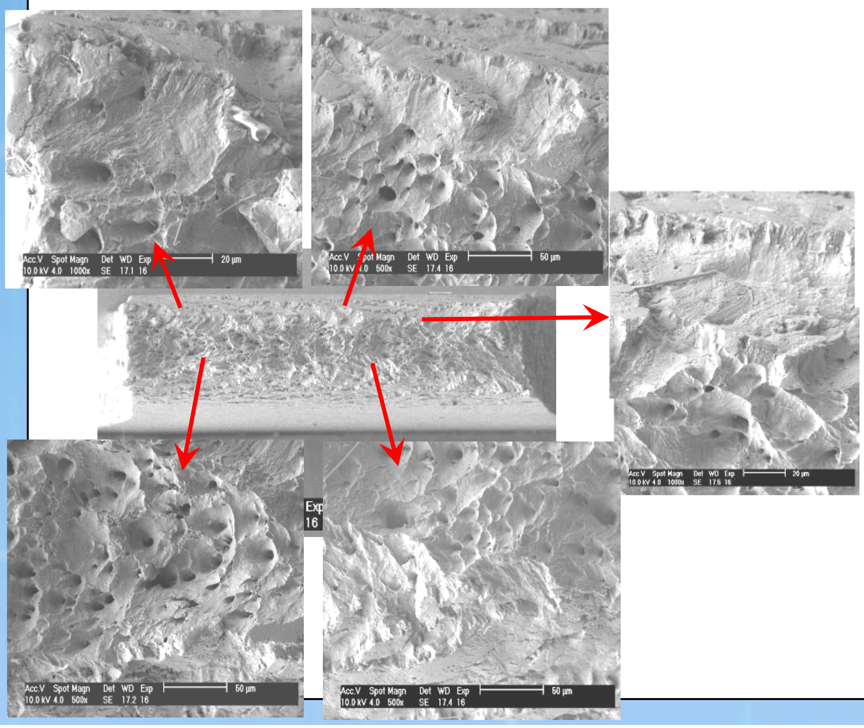

Ref: Y, Chen et al., NUREG/CR – 7018(2010) and 6965 (2008)

- Fracture morphology was unchanged with increasing dose from 10 to 48 dpa. Dimples remain the dominant features on failure surface.
- RA was similar to that of 10-dpa, ~60% for high-O, and ~80% for low-O specimens.

Results Obtained from CASS Samples

Fracture toughness results

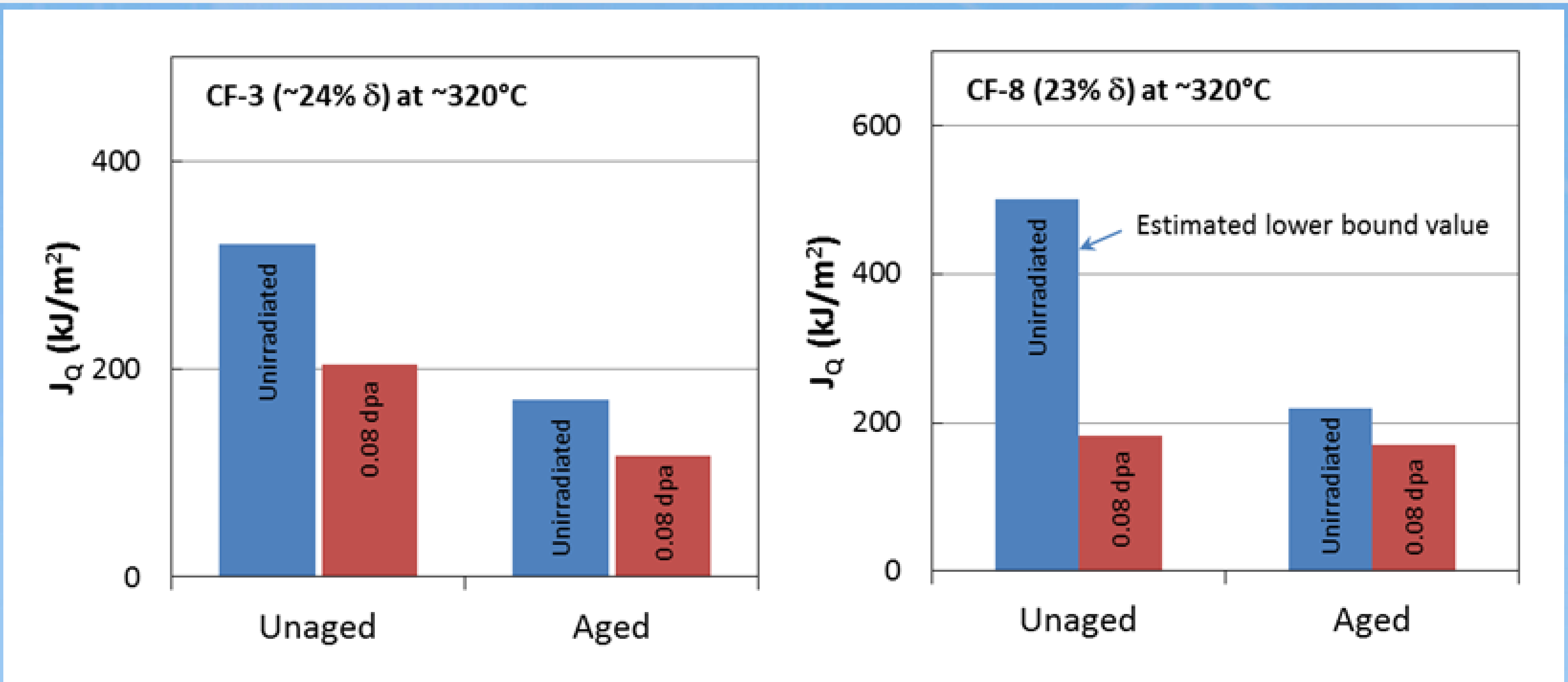

Ref: Y. Chen et al., NUREG/CR – 7084(2015)

- Neutron irradiation reduced fracture toughness (J_Q) in both unaged and aged CASS alloys.
- The decreases in J_Q were much more significant in the unaged samples, suggesting a dominant role of irradiation in causing embrittlement.

J versus crack extension as a function of irradiation for CASS

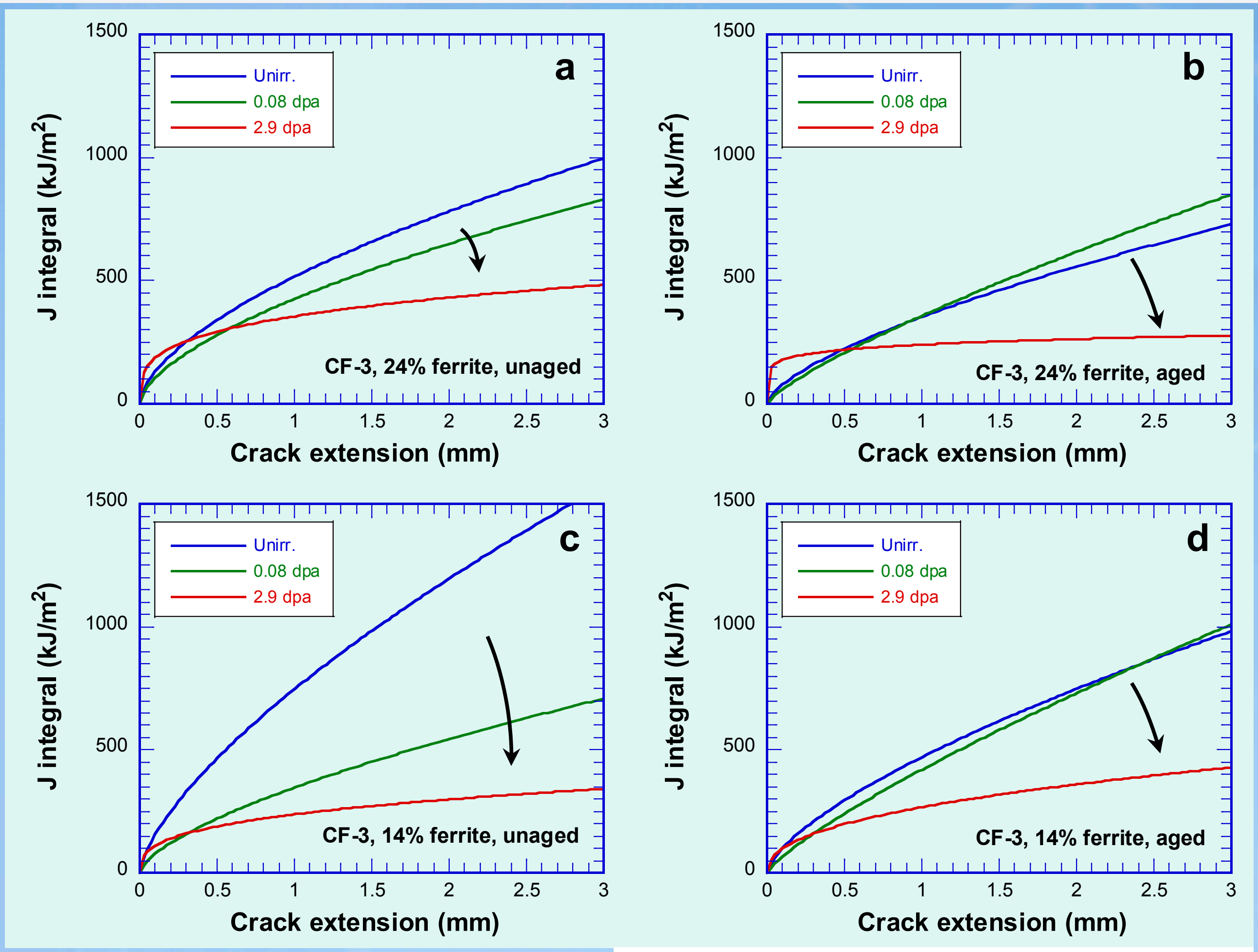

Ref: Chen et al., Env. Deg. Conf., 2017

- Decreased resistance in crack propagation in 2.9-dpa samples

U.S.NRC
UNITED STATES NUCLEAR REGULATORY COMMISSION
Protecting People and the Environment

Recent NRC Research on RPV Internals

– TEM analysis of the microstructure of irradiated stainless steels and CASS

TEM obtained from irradiated 304 SA stainless steel

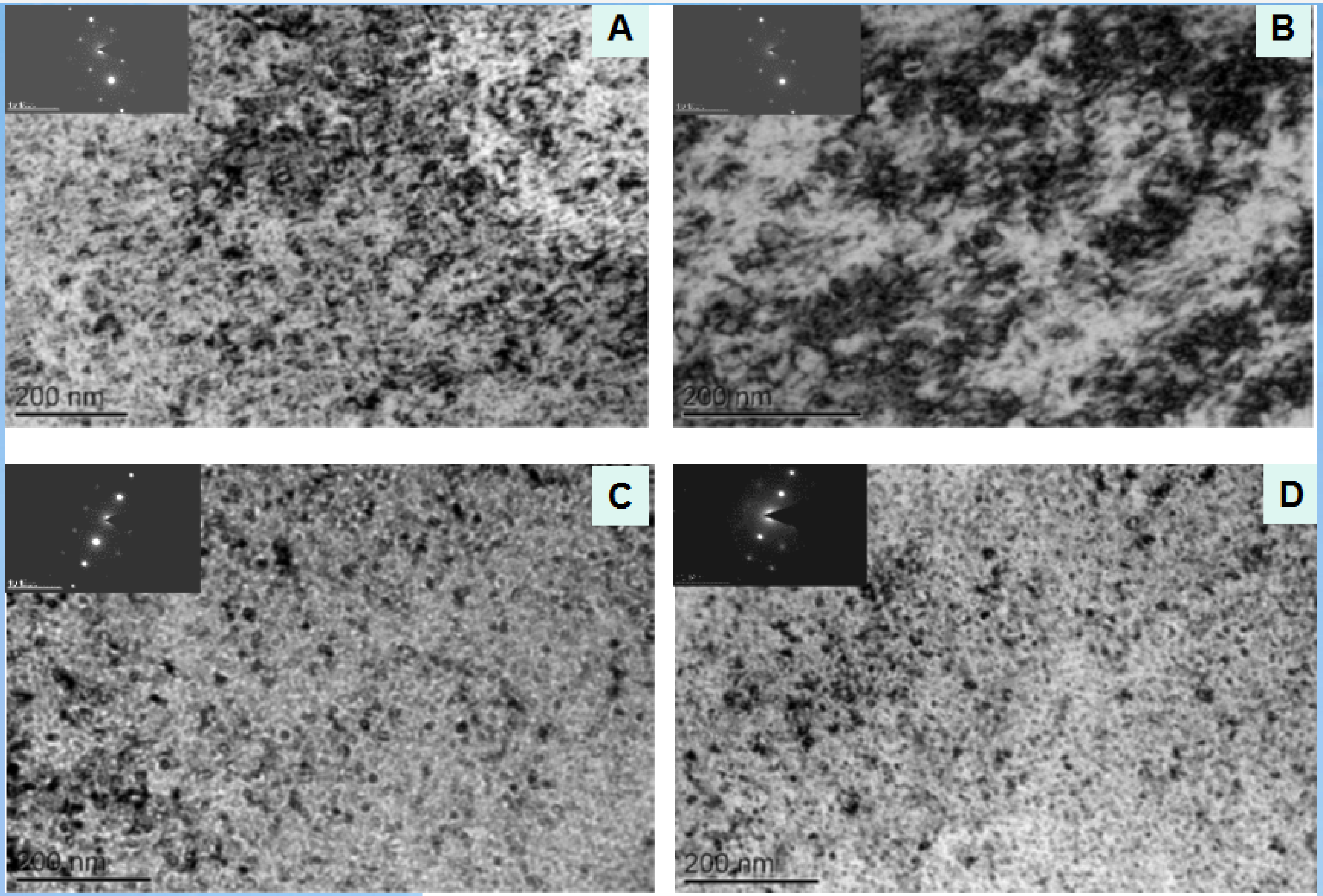

Ref: Yong et.al., To be published in J. Nucl. Mater., (2017)

Bright field imaging of dislocation loops at g020 for 20 dpa (A) and (B), g011 for 20 dpa(C) and (D). g011 for 40 dpa. ***Note: 'g' refers to electron beam orientation.***

Defect size and density of irradiated 304 SA – high sulfur stainless steel

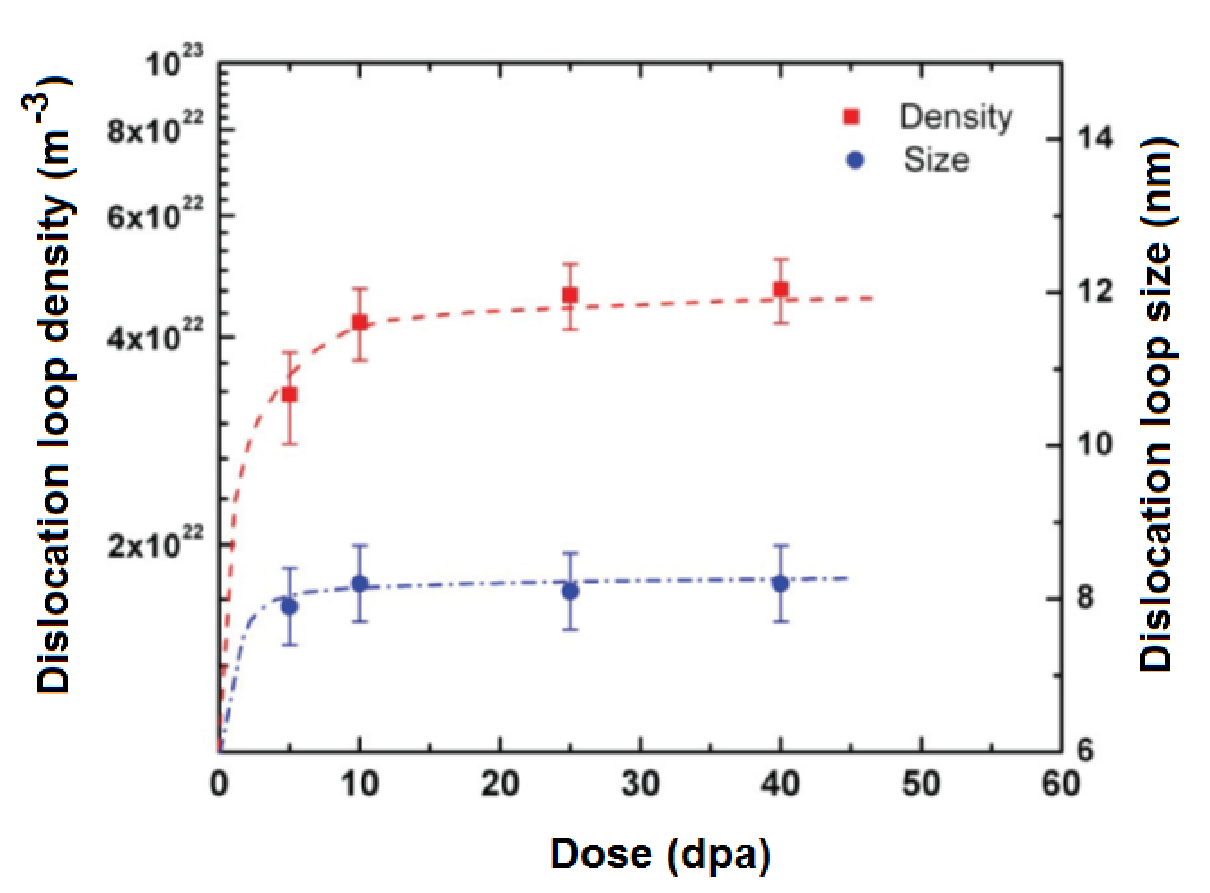

Ref: Chen et al., JNM, 466 (2015) 560

Density and average size of Frank loops represented as a function of neutron dose (dpa) for irradiated 304 SA-High S stainless steel

U.S.NRC
UNITED STATES NUCLEAR REGULATORY COMMISSION
Protecting People and the Environment

TEM observation: Effect of irradiation

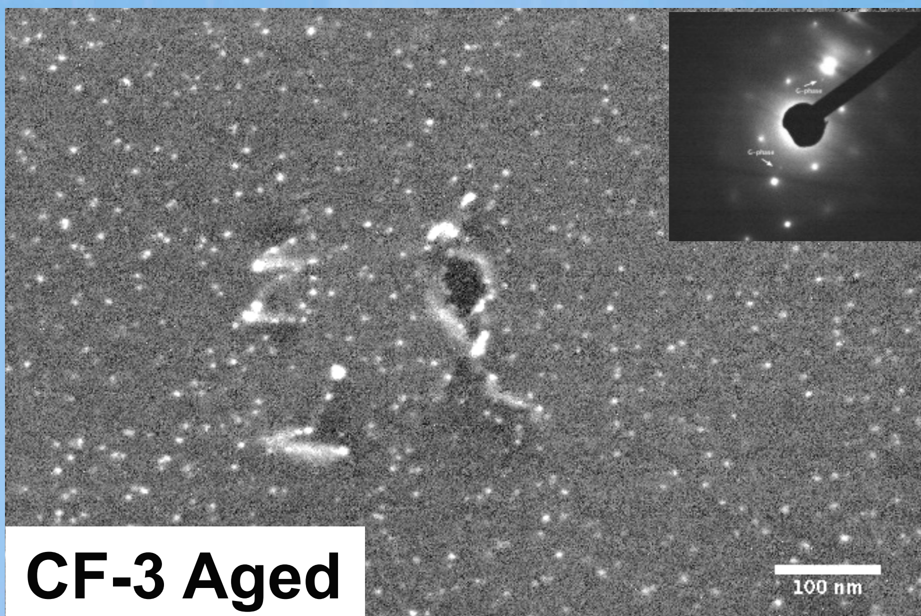

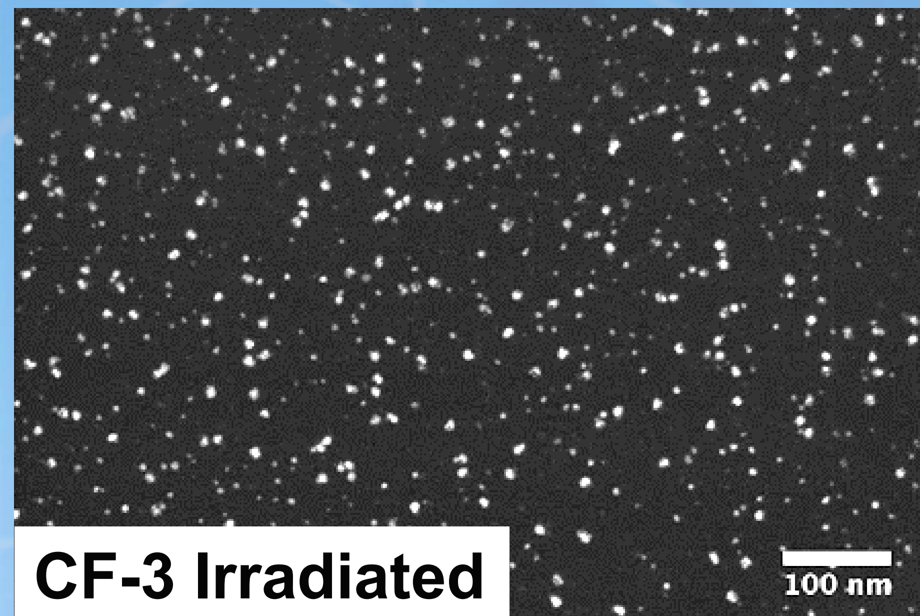

Ref: Chen et al., JNM, 466 (2015) 560

- Thermal aging and neutron irradiation resulted in similar precipitation microstructure.

TEM of irradiated CASS

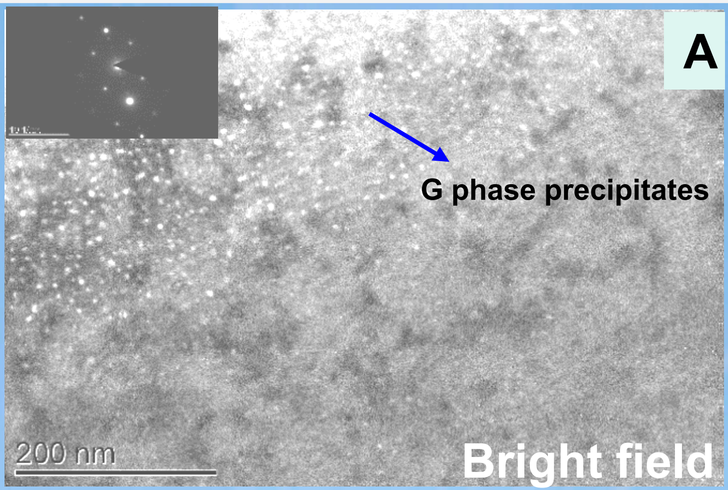

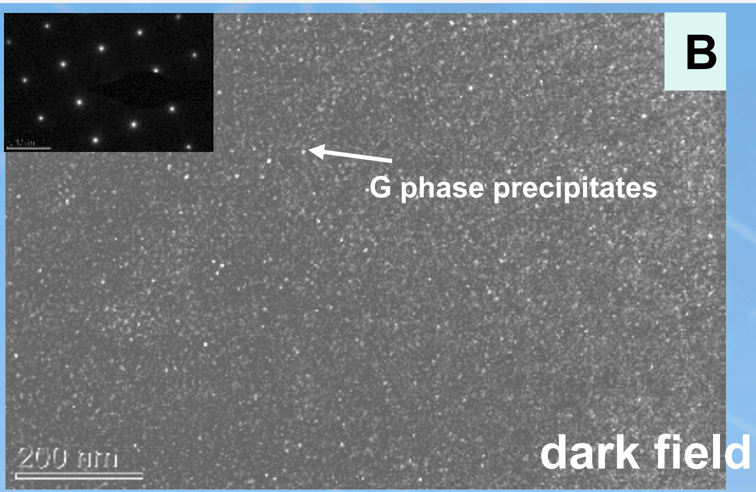

Dark field images of G phase precipitate at g-020(A) and exact zone axis(B) at [001] for 20 dpa irradiated CASS

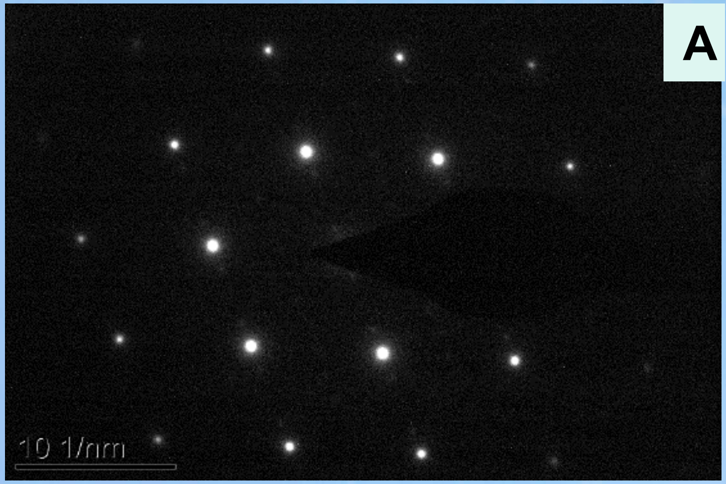

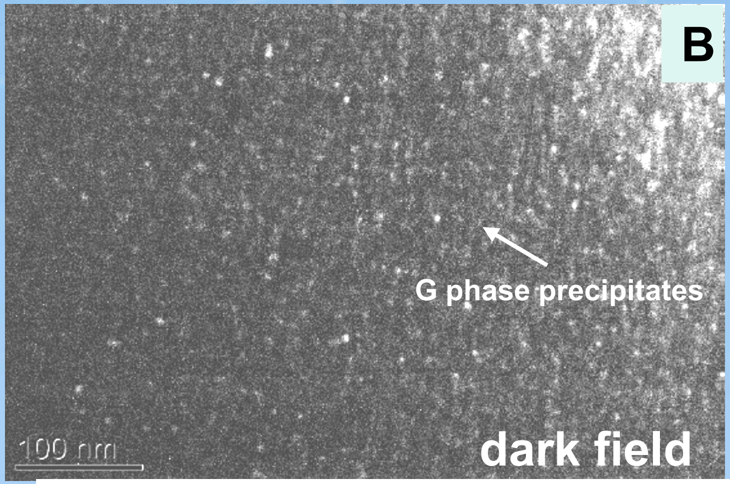

Ref: Chen et al., JNM, 466 (2015) 560

Diffraction pattern (A) and dark field (B) of G phase precipitate at [013] for 40 dpa irradiated CASS

TEM of irradiated CASS (cont.)

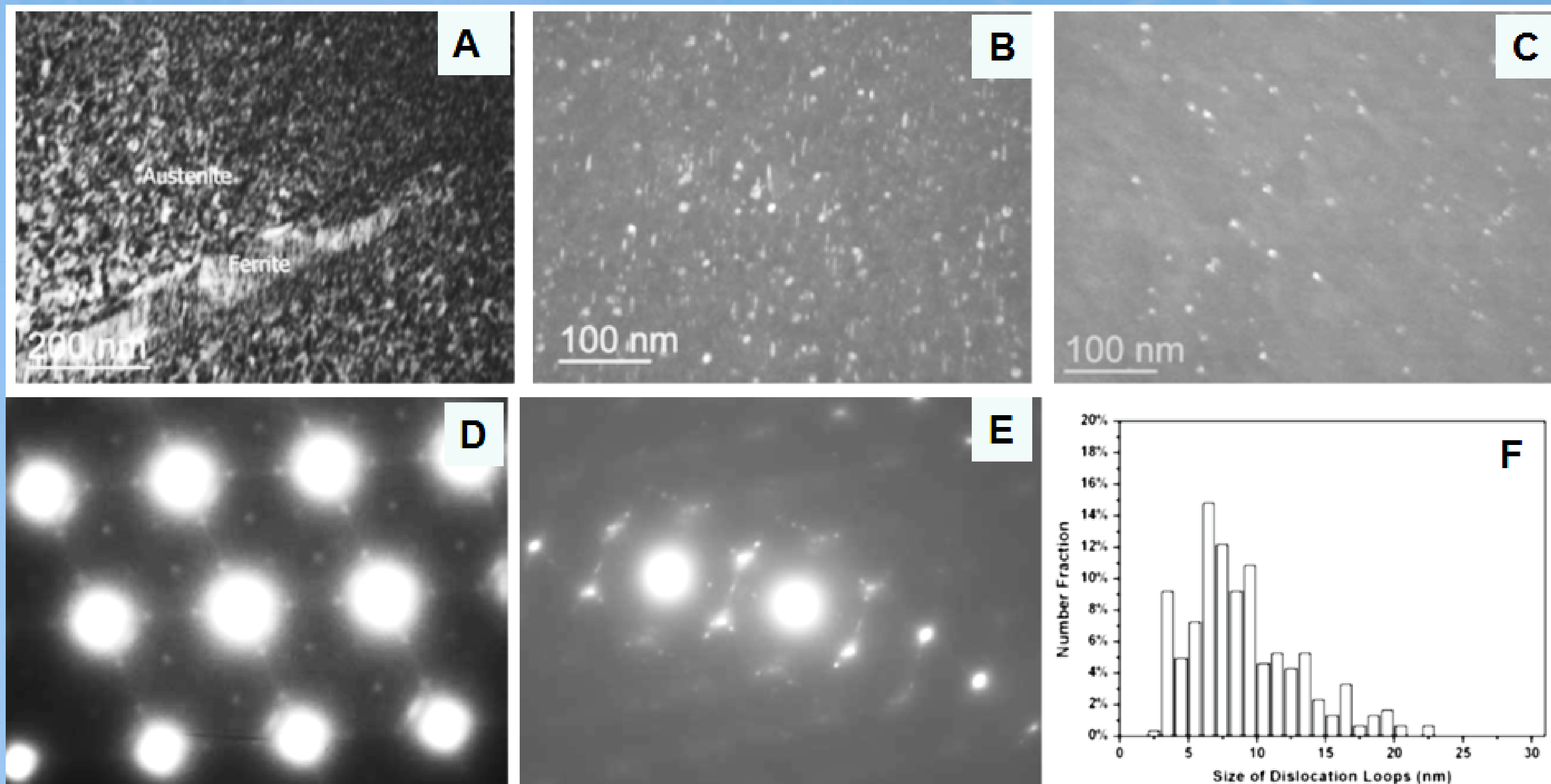

Transmission electron micrographs obtained from CF-8 grade CASS. The micrographs were obtained with the beam direction B close to <110>: (A) BF field image of austenite and ferrite phases, (B) Relrod DF image of dislocation loops, (C) dark filed image of the fine precipitates in austenite grain using the ultra-reflections in (D), and (D) diffraction patterns showing the coherence of the precipitates with the matrix, (E) diffraction patterns showing the reflection streaks arising from dislocation and (F) the size distribution of dislocation loops.

Ref: Chen et al., JNM, 466 (2015) 560

TEM of He-ion implanted nickel-helium bubbles

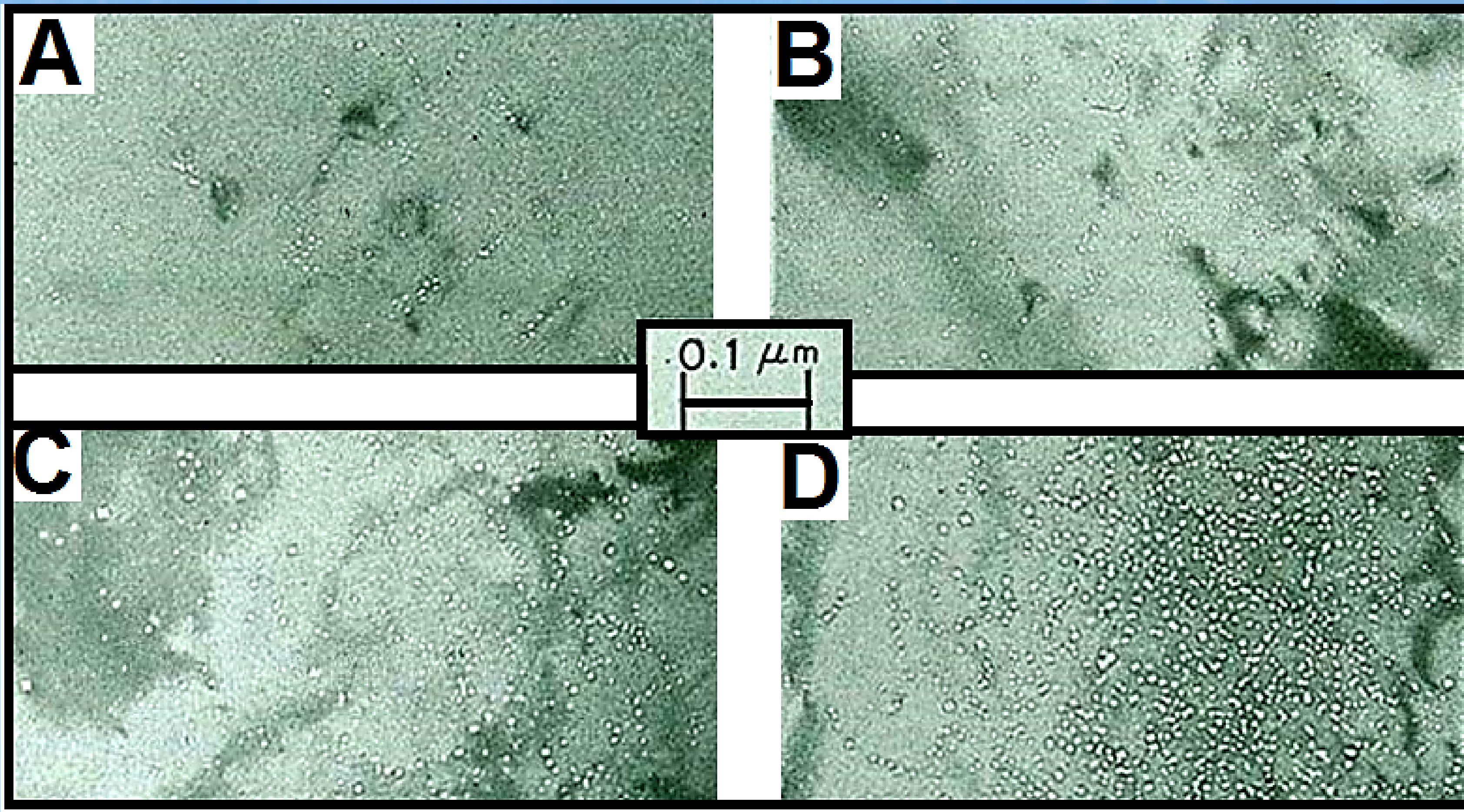

Increasing helium ion dose A → B → C → D

Ref: Das et al., J. Nucl. Mater., 1977

TEM of He-ion implanted molybdenum-helium bubbles

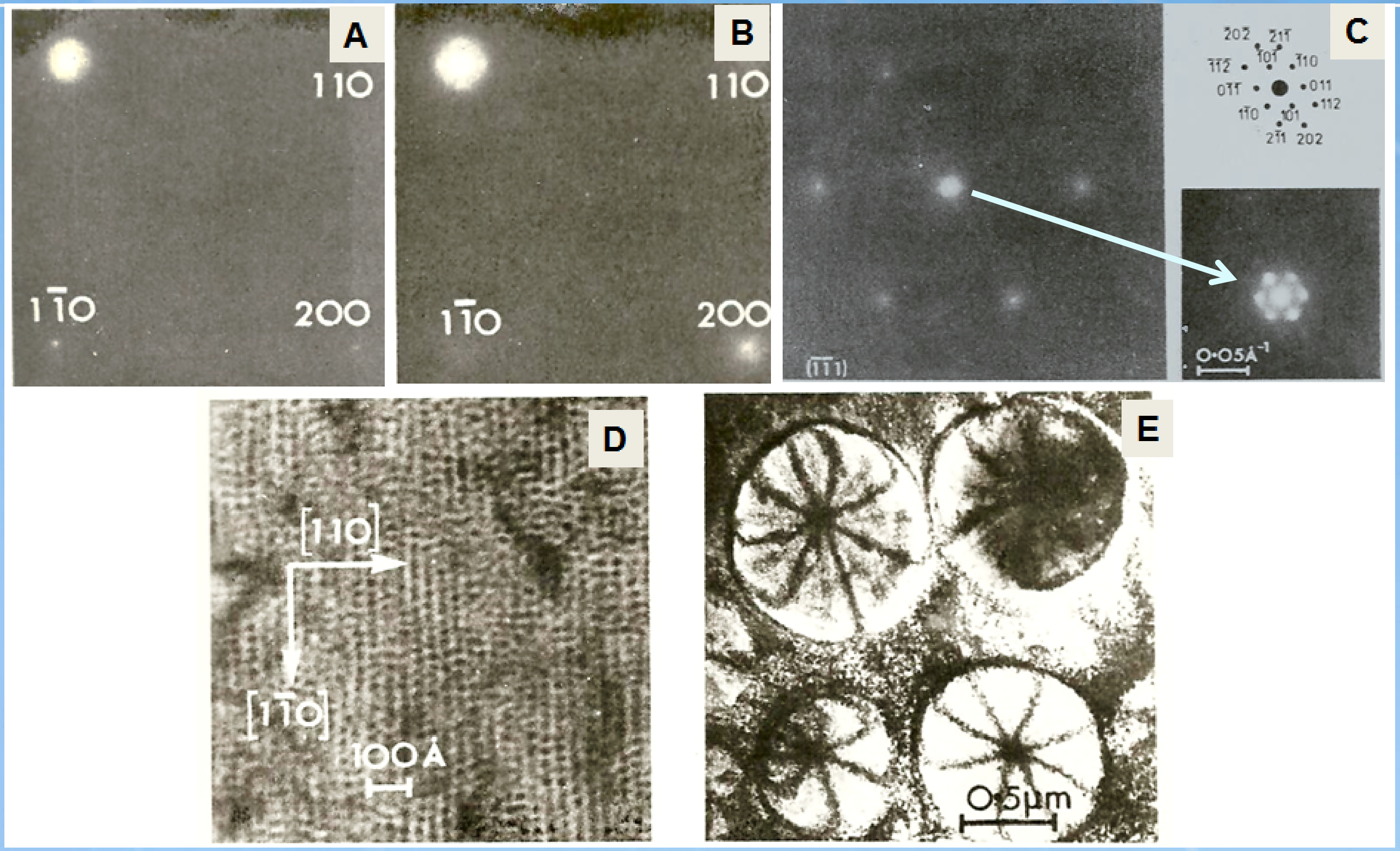

(A) Diffusion ring produced around the (000) matrix reflection of a (001) sample by diffraction from helium bubbles. Irradiated at 250°C with 25 keV He^+ ions. (B) As far (A) after further irradiation. Four bubble super lattice reflection appear with in the ring. Ion dose 4.5 X 10^{17} He^+ ions/cm^2. (C) Bubble super lattice reflections around the bcc matrix reflection in a (111) sample. Insert is the enlargement of (000) region shows faint second order reflections. Dose 2X 10^{17}- 40 keV He^+ ions/cm^2 at 400°C. (D) Transmission electron micrograph showing alignment of helium bubbles in (001) molybdenum sample. Dose 2X 10^{17}, 40 keV He^+ ions/cm^2 at 400°C. (E) Transmission electron micrograph of surface blistering in molybdenum after bombardment with 10 keV He^+ to a Dose of 2X 10^{17} ions/cm^2 at 400°C. [Ref: Mazey etal., J. Nucl. Mater., 64,145 (1977).

Atom Probe Tomography (APT)

Atom probe tomography

- **What are these precipitates/phases:**
  - ➔ **APT will tell the**
    - **compositional change**
    - **location of the elements**

Example – segregation of chromium

– depletion of a specific elemental constituent

APT Analysis: Cr map

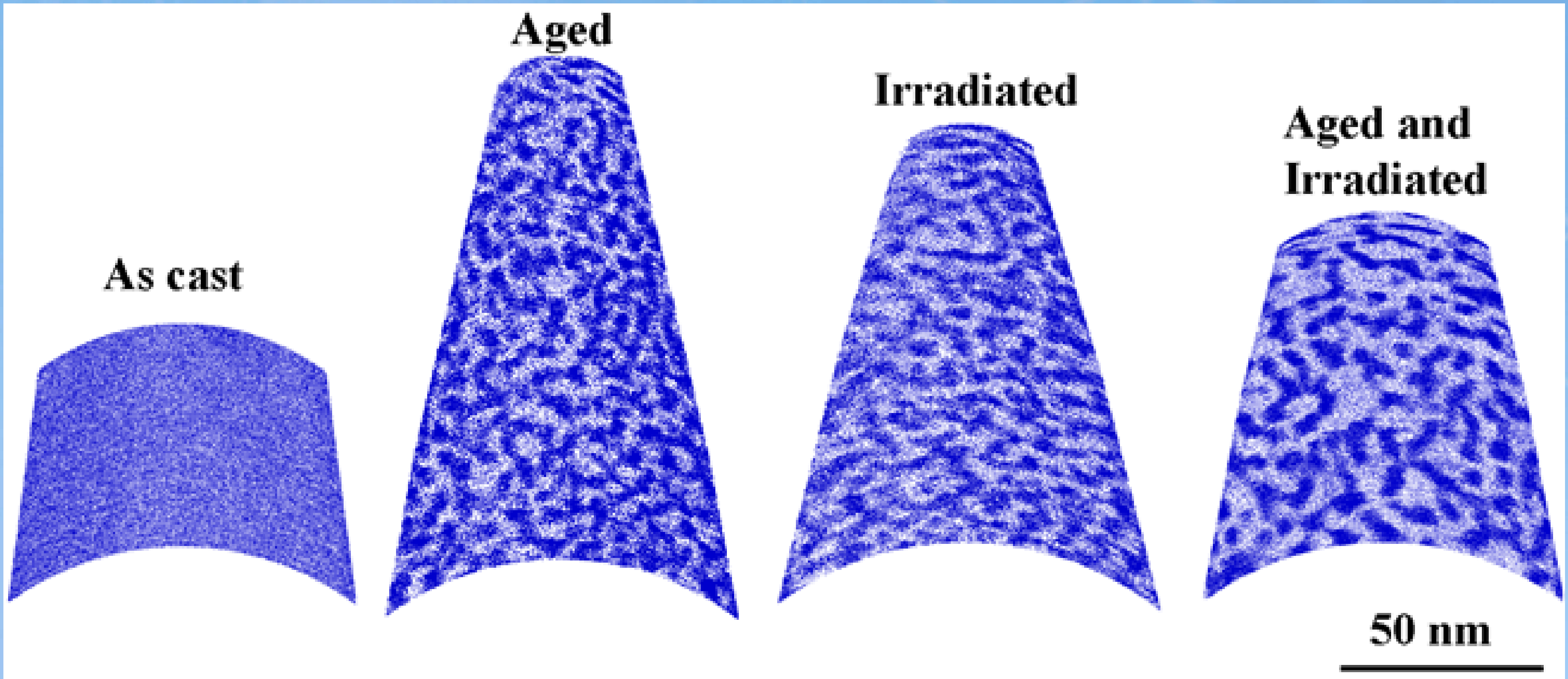

Ref: Li et al., JNM, 466, 201 (2015)

- Irradiation and thermal aging resulted in similar segregations of Cr and Fe (α/α' decomposition).
- The extent of segregation was more evident in the irradiated samples with prior aging.

APT Analysis (cont.): Aged, irradiated stainless steel and CASS samples

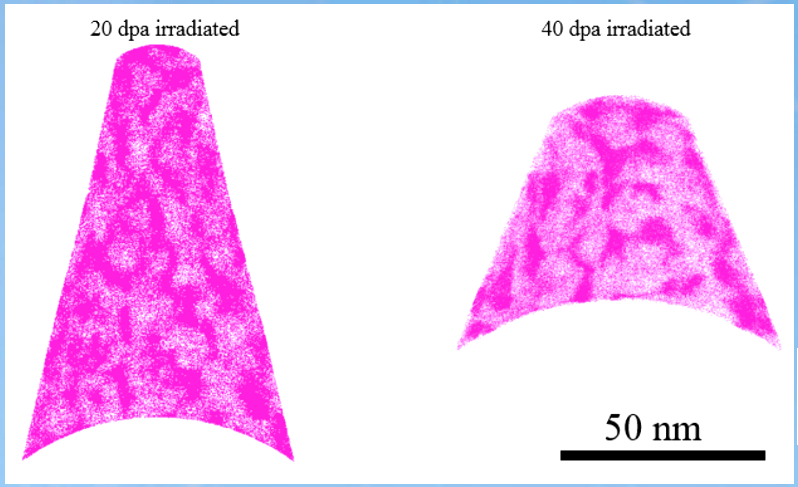

Ref: Yong et al., To be published in J. Nucl. Mater., (2017)

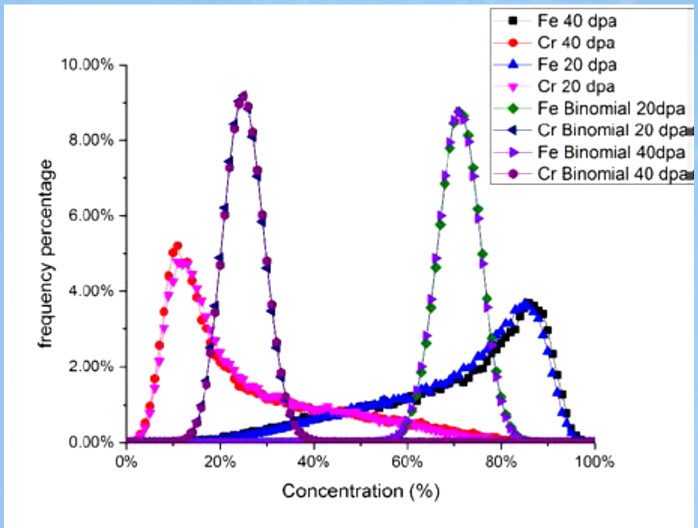

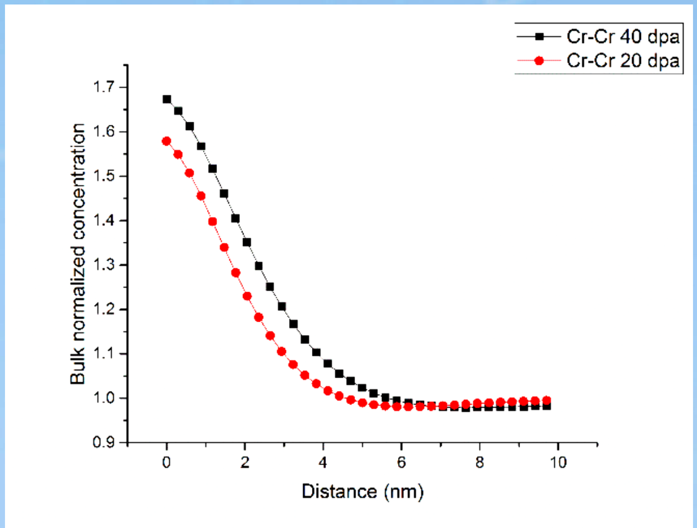

Cr Fe frequency distribution (a) and Radial distribution functions (b) of Cr-Cr ions in irradiated at 20 and 40 dpa CF-3.

APT Analysis (cont.): Aged, irradiated CASS samples

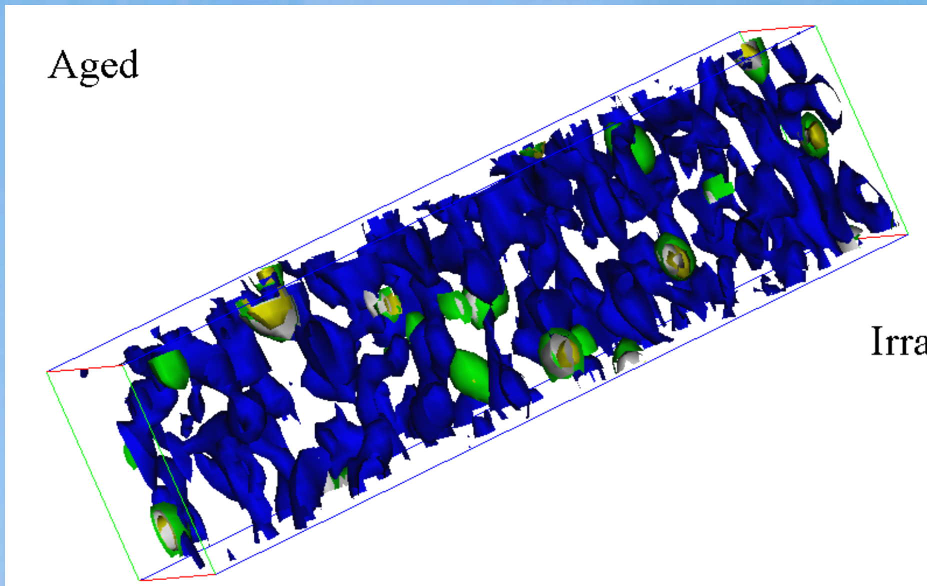

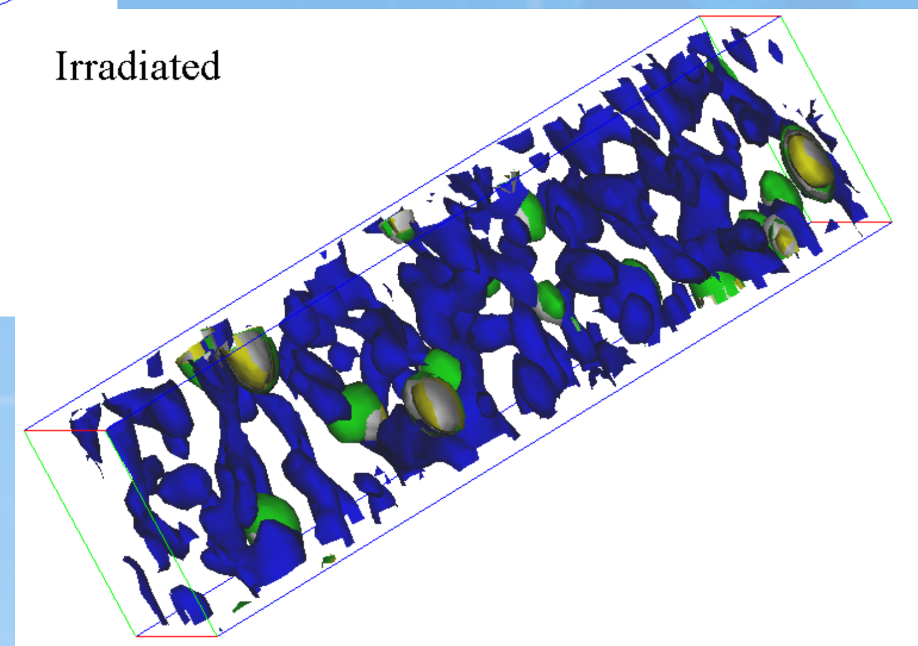

Ref: Yong et al., To be published in J. Nucl. Mater., (2017)

Iso-surfaces of Mn(Gold)-Ni(Green)-Si(Gray) clusters and interfaces of Cr (Blue) enriched α' phases: Aged(33.58%Cr-7.47%Mn-13.39%Ni-5.6%Si) and Irradiated (33.57%Cr-6.72%Mn-14.31%Ni-

U.S.NRC
UNITED STATES NUCLEAR REGULATORY COMMISSION
Protecting People and the Environment

High Energy X-ray Data Processing and Analysis

U.S.NRC
UNITED STATES NUCLEAR REGULATORY COMMISSION
Protecting People and the Environment

Microstructure – property correlation

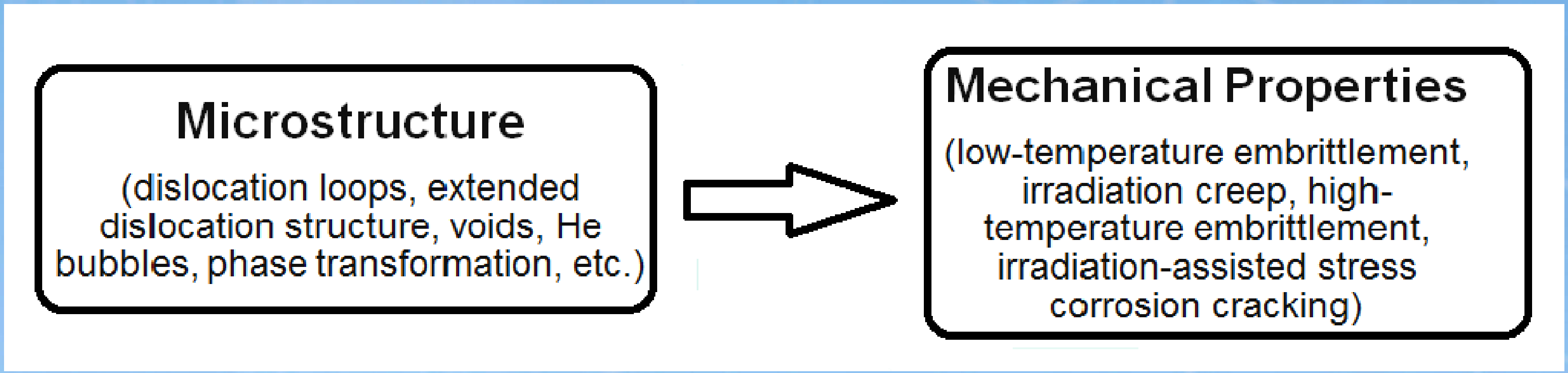

- **Why we want to correlate microstructure to mechanical properties:**
  - ➔ **Enable us to develop a predictive model**
    - **Example hardness to internal physical structure**
    - **Physical structural change relates to development of new stress**
    - **New Stress field can be modeled using finite element analysis (FEA)**
    - **FEA then can predict where failure can occur.**

Interface of *i*RadMat with beamline infrastructure

Simultaneous WAXS/SAXS measurement:

- ***In situ* with deformation.**
- **Wide-angle detector array** (1.0m - 4.5m downstream)
- **Small-angle detector** (6.6m downstream)

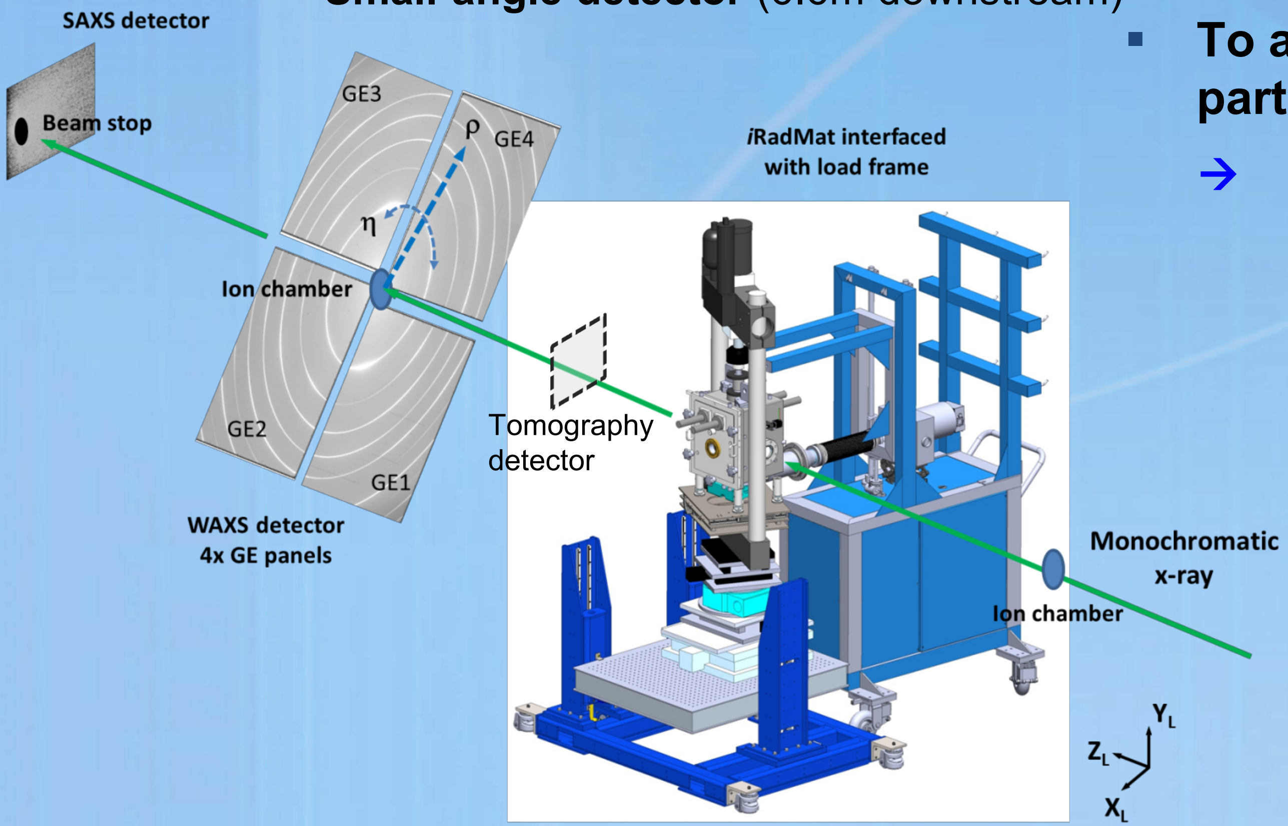

- **To analyze load partitioning among phases**
  - → **Ex. The role of ferrite in the hardening and embrittlement behavior of CASS.**

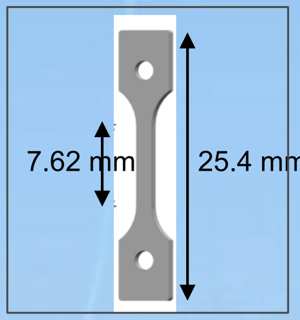

Note: WAXS : Wide angle x-ray scattering
SAXS: Small angle x-ray scattering

Ref: Zhang X *et. al.*, *submitted to* ***Review of Scientific Instruments (2017)***

U.S.NRC
UNITED STATES NUCLEAR REGULATORY COMMISSION
Protecting People and the Environment

High Energy X-ray Data Processing

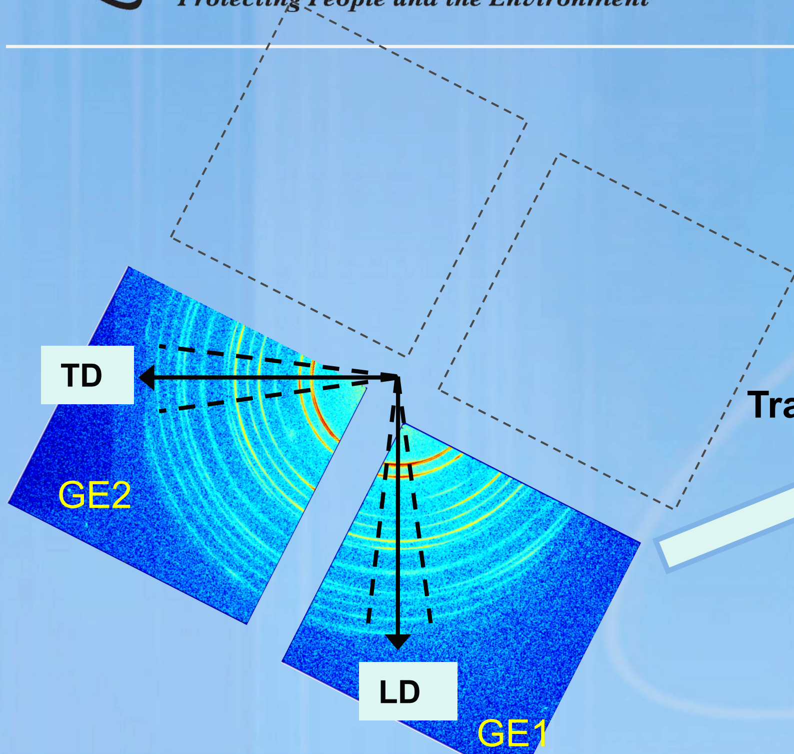

Transform

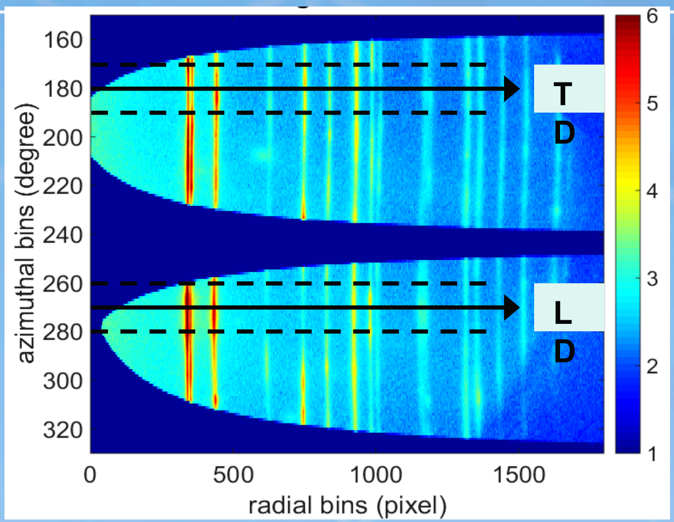

Integrate

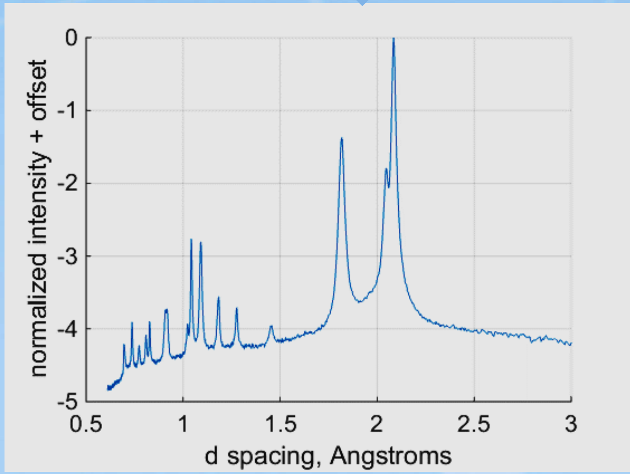

Peak fitting

- Phase identification
- Peak position → lattice strain
- Peak width → crystallite size & strain

Interpretation

Ref: Zhang X *et. al.*, *submitted to* ***Review of Scientific Instruments (2017)***

Analysis on 304L SS

- **Stainless Steel does not undergo thermal embrittlement.**
  - **Stainless steel is γ - austenite - with face centered cubic (fcc) structure**
- **304 Stainless Steel suffers from neutron embrittlement at higher neutron doses.**
  - **Increase in hardness (nano-indentation) suggests that 304 SS was embrittled**
  - **Such neutron embrittlement in stainless steel is due to structural change.**
- **What is the evidence of such structural change?**
  - **High energy XRD may provide some evidence**

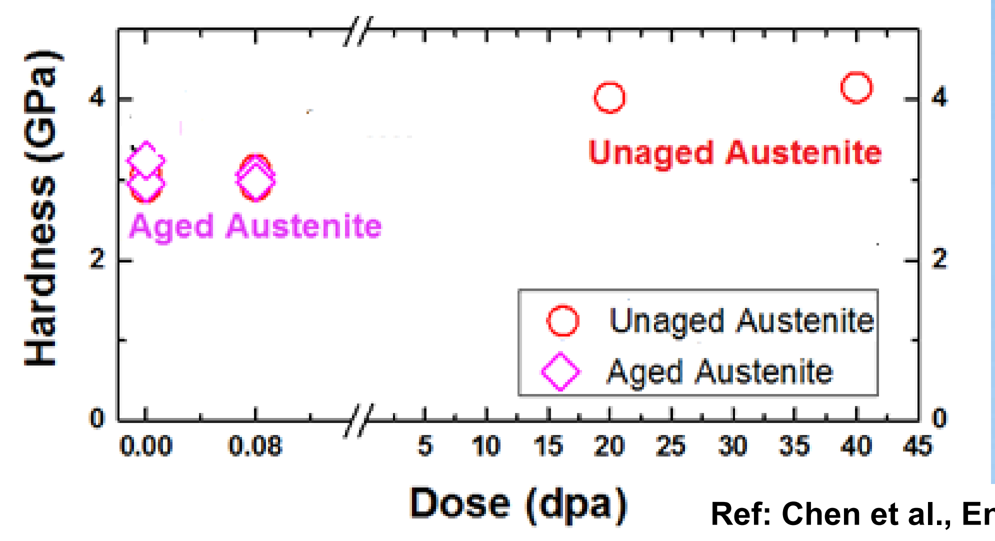

Ref: Chen et al., Env. Deg. Conf., (2017)

Deformation-induced martensitic transformation in 316 SS

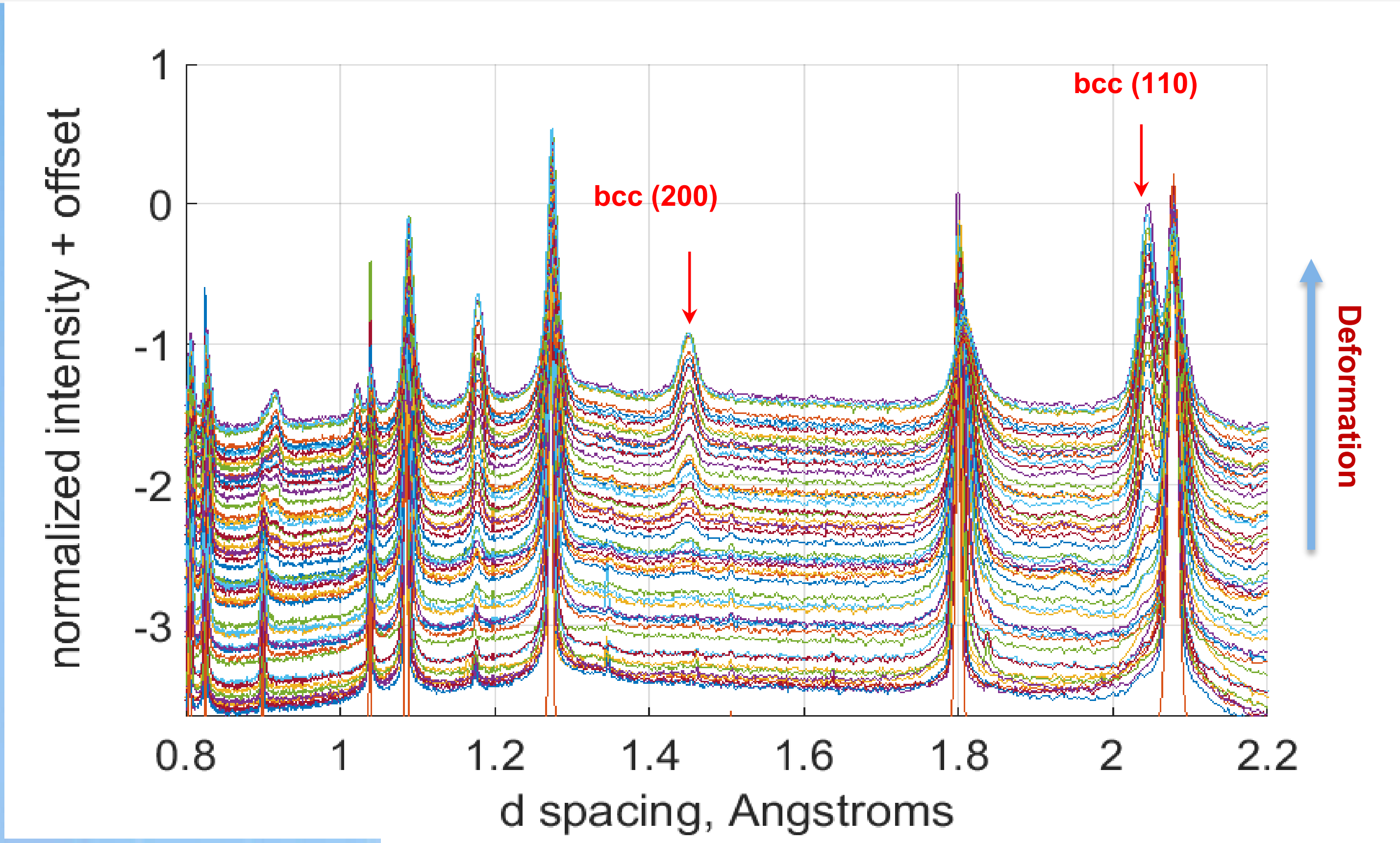

Ref: Zhang X *et. al.*, *submitted to* ***Review of Scientific Instruments (2017)***

- **XRD lineout shows increased ferrite/martensite fraction with deformation**
- Martensitic transformation is one of the hardening mechanisms (besides work-hardening) in the deformation of un-irradiated 316 SS.

Analysis of CASS Nano-hardness

Cast Austenitic Stainless Steels (CASS)

- CASS ➢ Dual-phase microstructure of δ - ferrite and γ-austenite

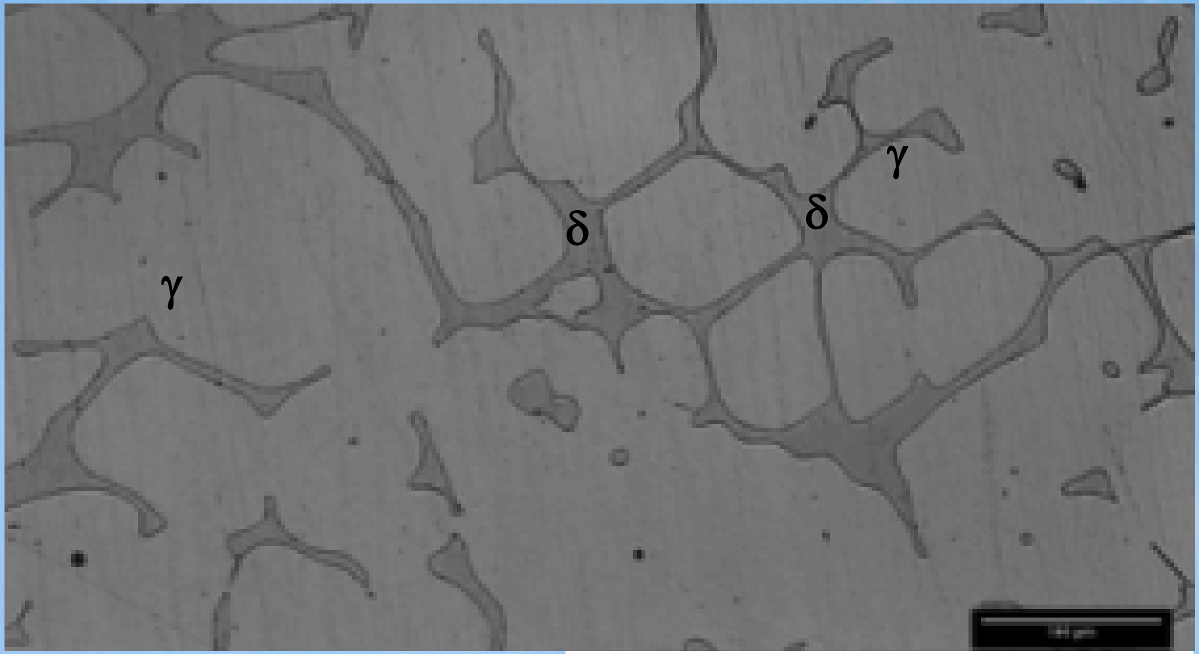

Ref: S.A. David, et al, JOM, June, 2003.

- **Beneficial effects of delta ferrite**
  - Help prevent "hot cracking"
  - Provide strength (Hardness of δ - ferrite > γ-austenite)
  - Improve sensitization and SCC resistance

Nano-indentation test to distinguish the response of ferrite and austenite

- **Need to separate the different mechanical responses of ferrite and austenite**
- **Nano-indentation is a surface measurement**

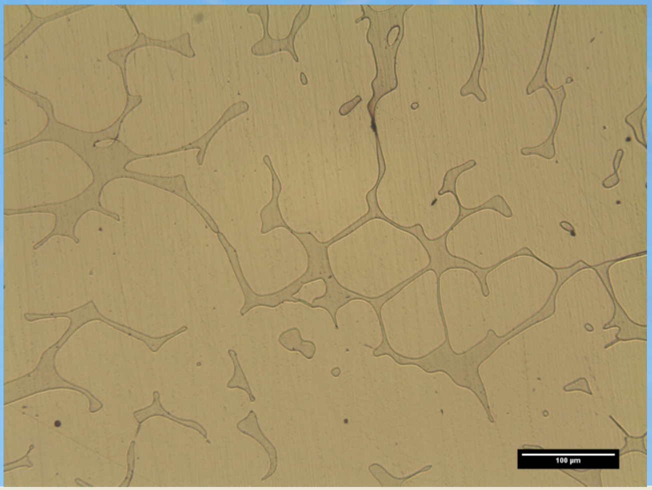

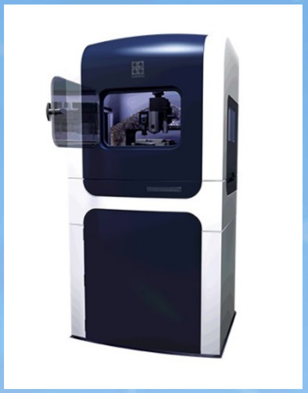

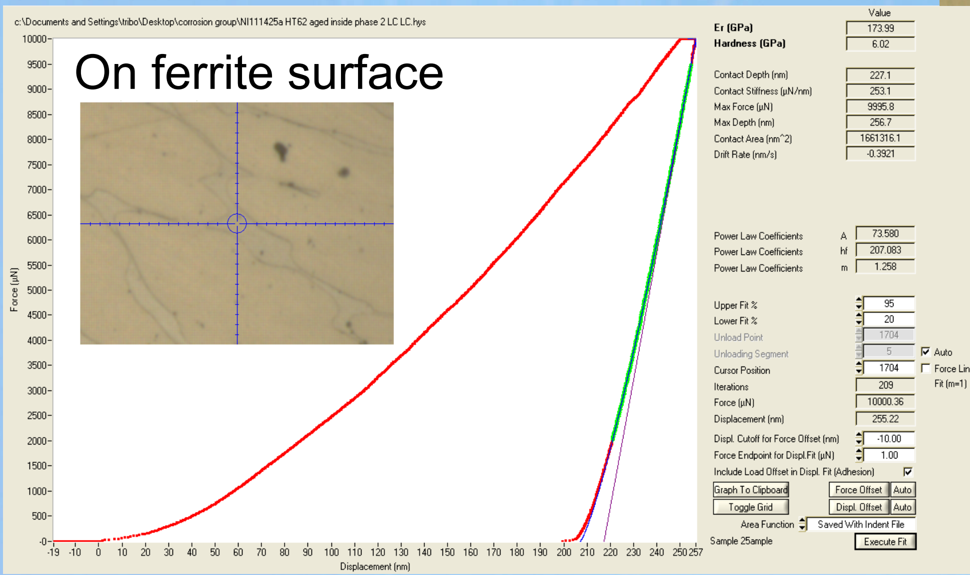

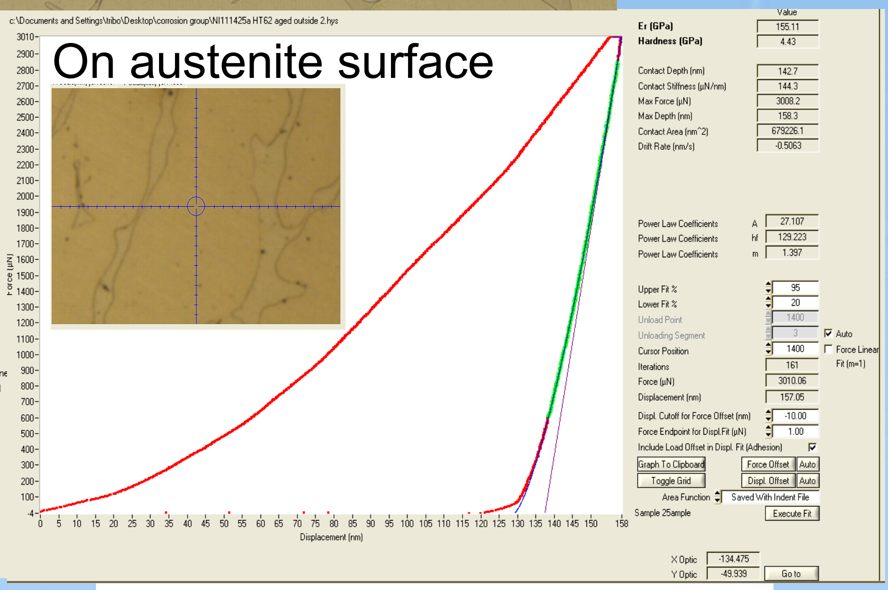

Ref: Chen et al., Env. Deg. Conf., (2017)

Nano-indentation Tests on CASS - Effect of irradiation

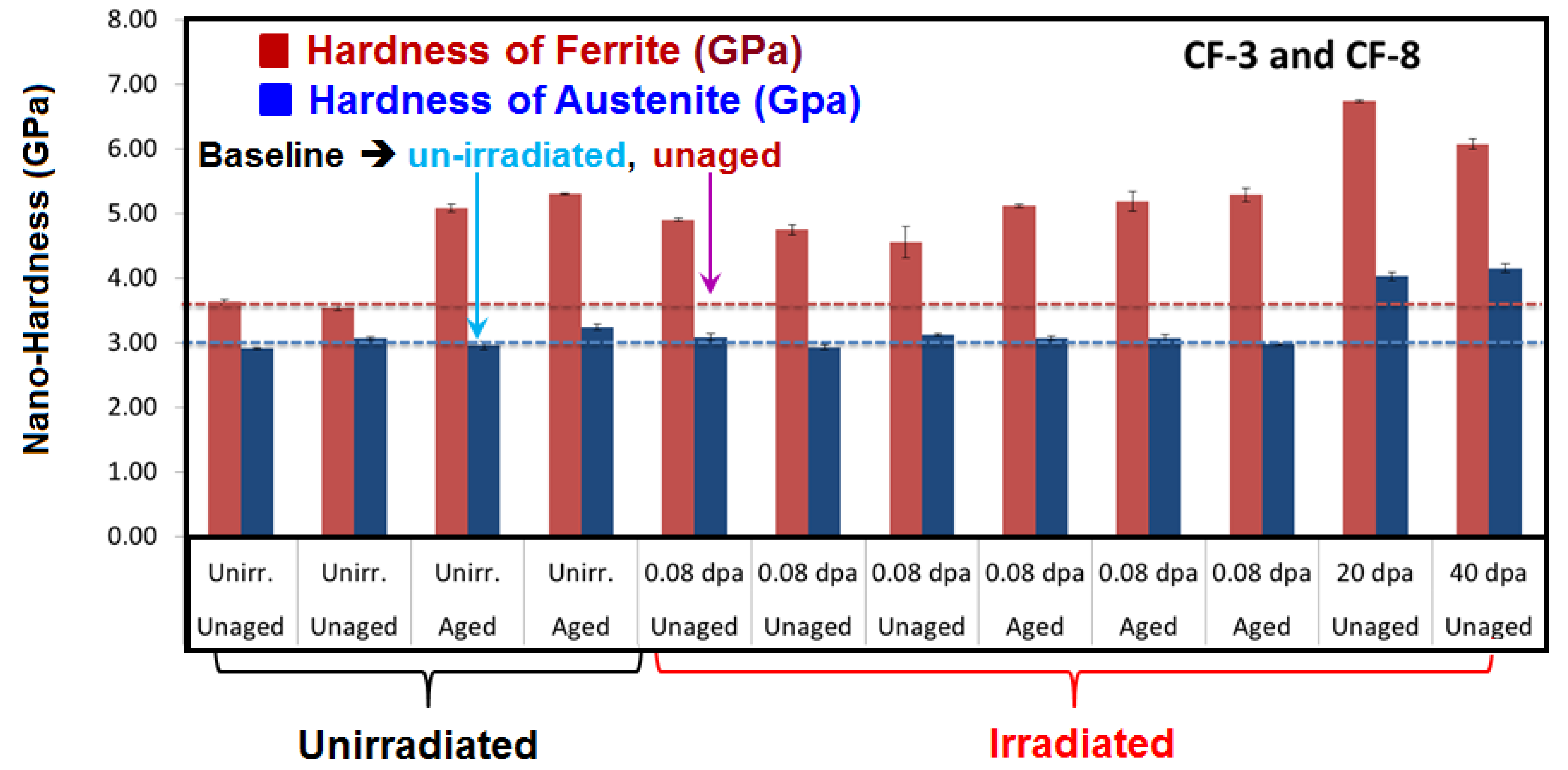

Ref: Chen et al., Env. Deg. Conf., (2017)

In-situ tensile tests on CASS (CF-8, 23% δ) at RT

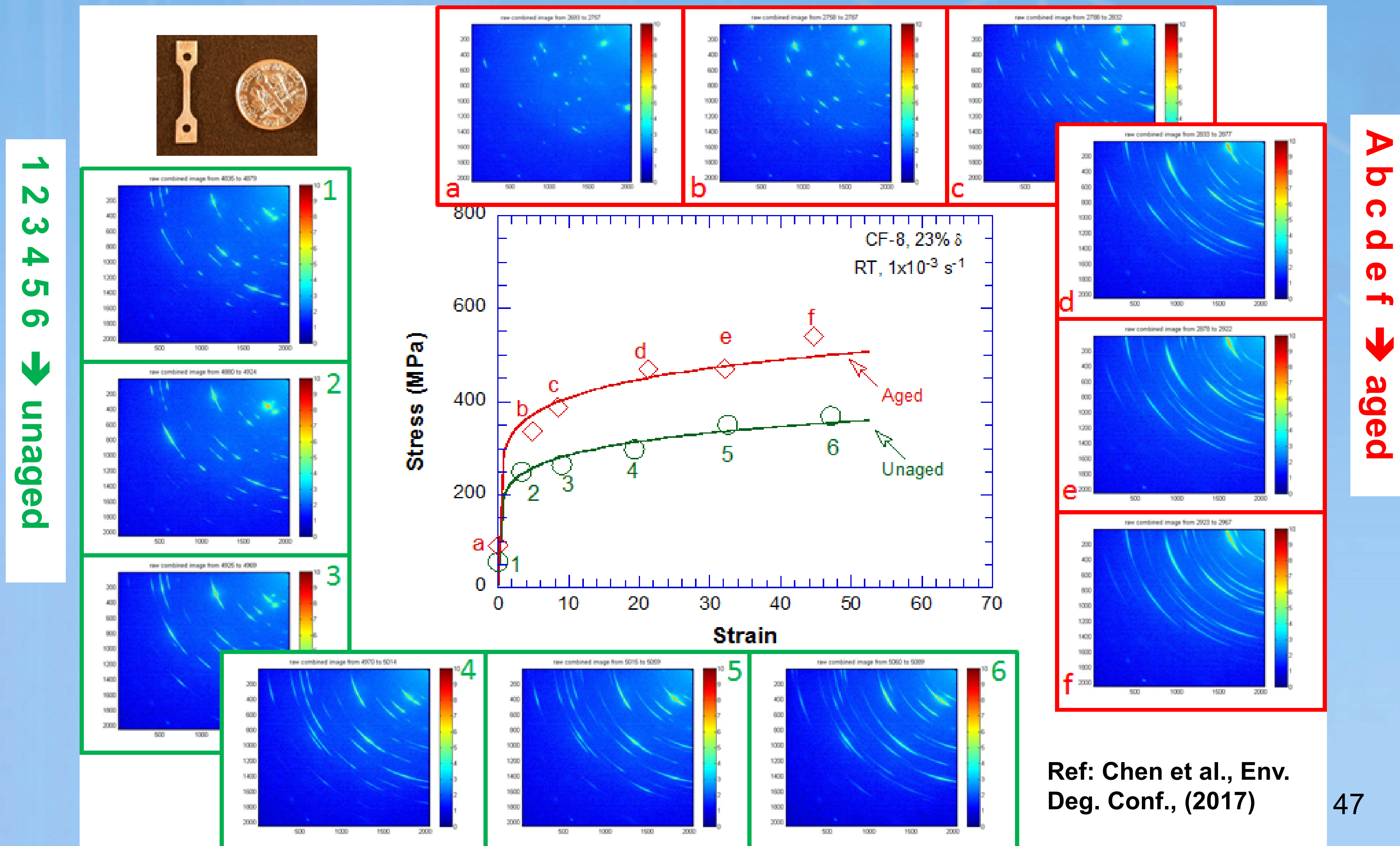

Ref: Chen et al., Env. Deg. Conf., (2017)

WAXS Results on Unaged and Aged 23% ferrite (CF-8) CASS CF-8

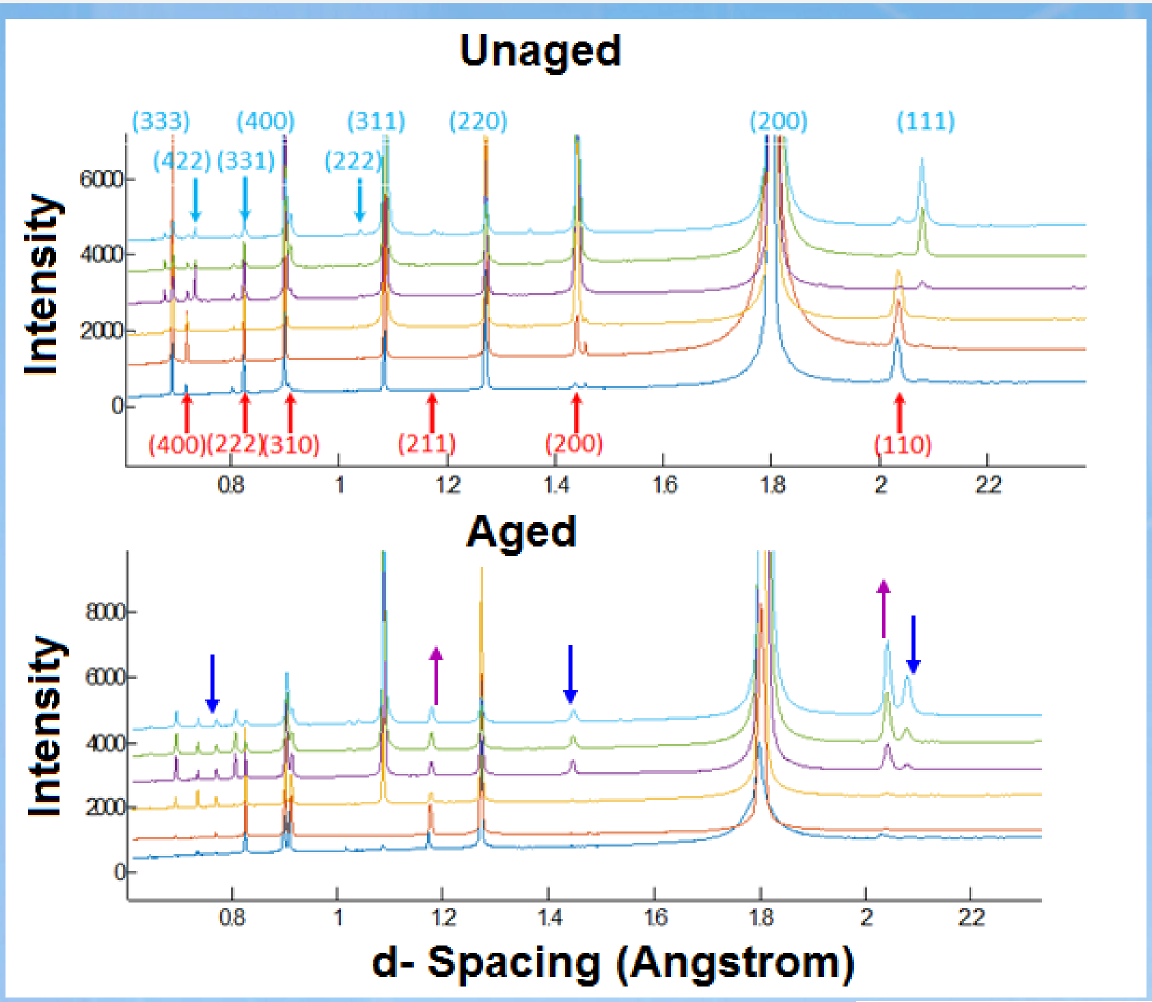

Ref: Chen et al., Env. Deg. Conf., (2017)

Blue arrow represent **decrease** in peak intensity
Red arrow represent **increase** in peak intensity

CASS (CF-8 with 23% - δ - ferrite, unaged vs. aged

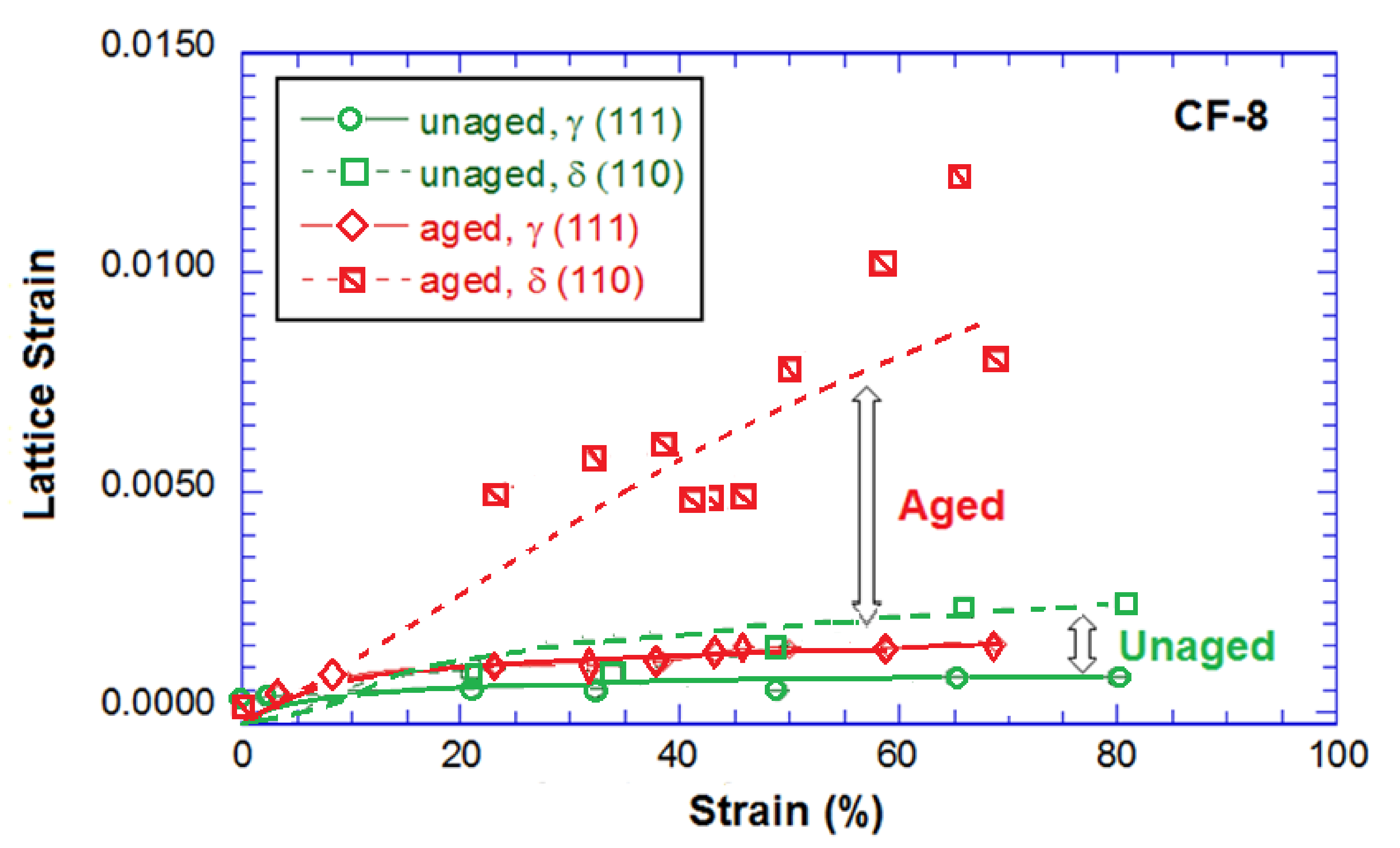

Ref: Chen et al., Env. Deg. Conf., (2017)

Analysis of high energy XRD results

- **High energy XRD provides the information on the distribution of structural changes along the sample during deformation.**
  - **That is whether the deformation is uniform or not.**
  - **If the deformation is not homogenous, is there any change in the grain morphology?**

- **Preliminary investigation suggests that inhomogeneity is directly related to the grain size changes during deformation.**
  - **(Ex. Next slide)**

Note: More research is needed to establish this conclusion

Inhomogeneous deformation in irradiated sample

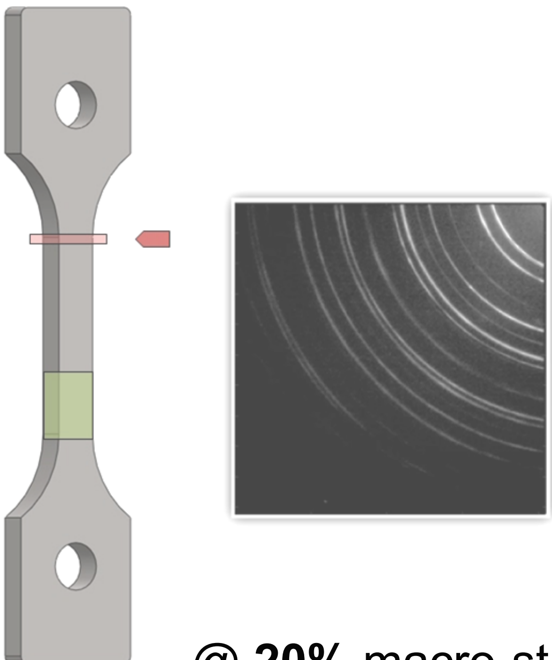

@ **20%** macro-strain

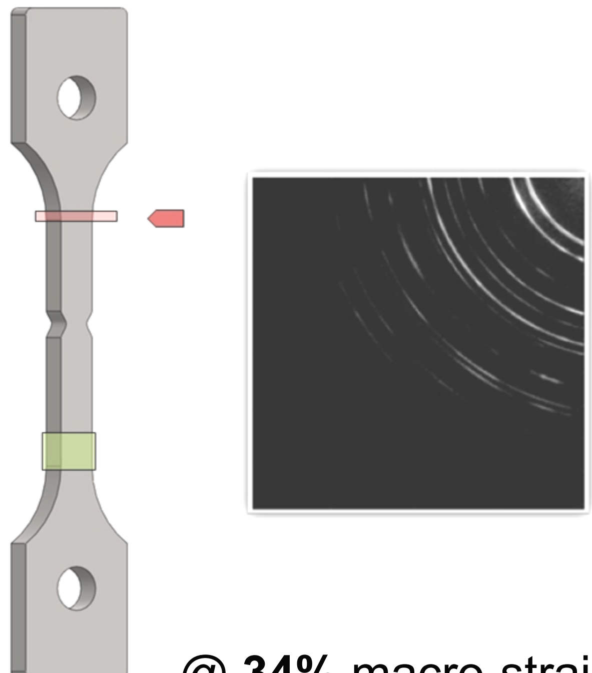

@ **34%** macro-strain

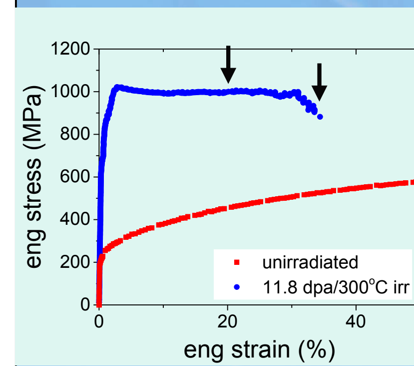

Observations:

- **Deformation starts from the top and propagates to the bottom (Lüders Band).**
- **Necking occurred before band fully propagating through.**
- **Heavier deformation leads to heavier texture and more phase transformation.**

Ref: Zhang X *et. al.*, *submitted to* ***Review of Scientific Instruments (2017)***

High-energy X-ray diffraction microscopy (HEDM)

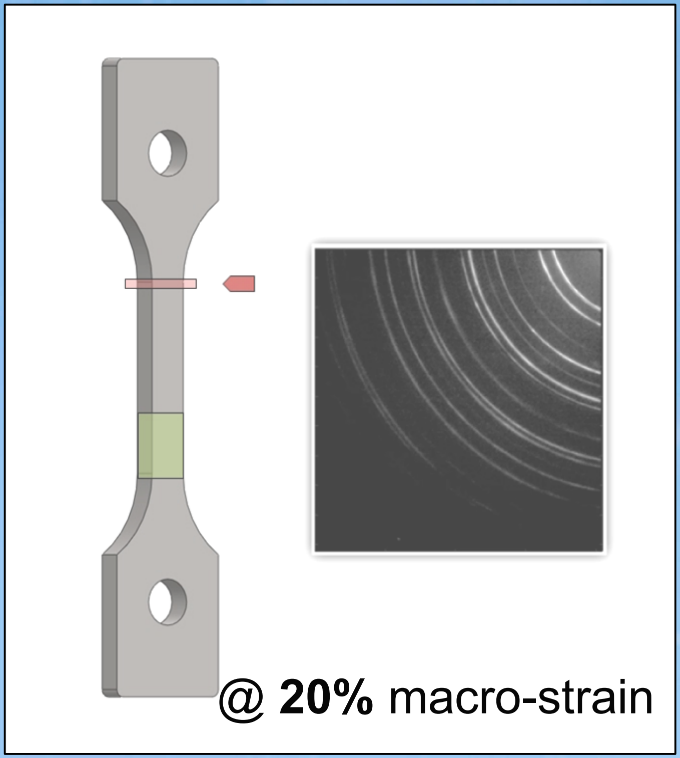

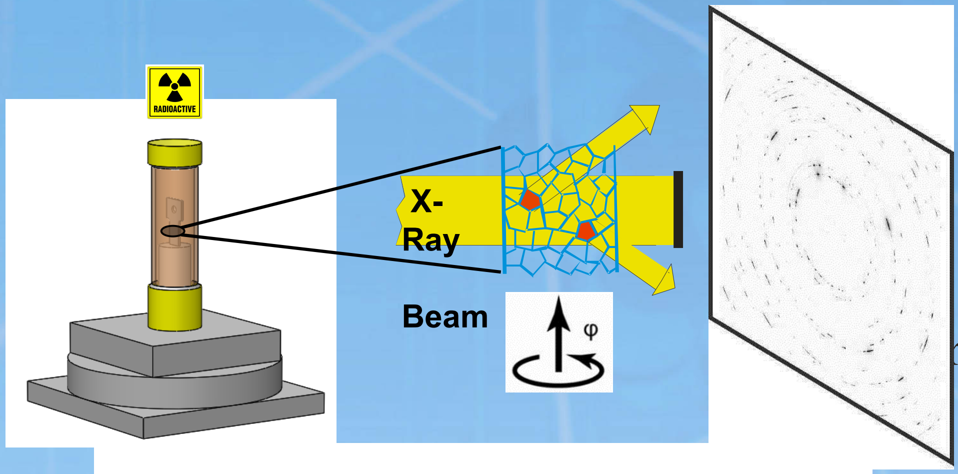

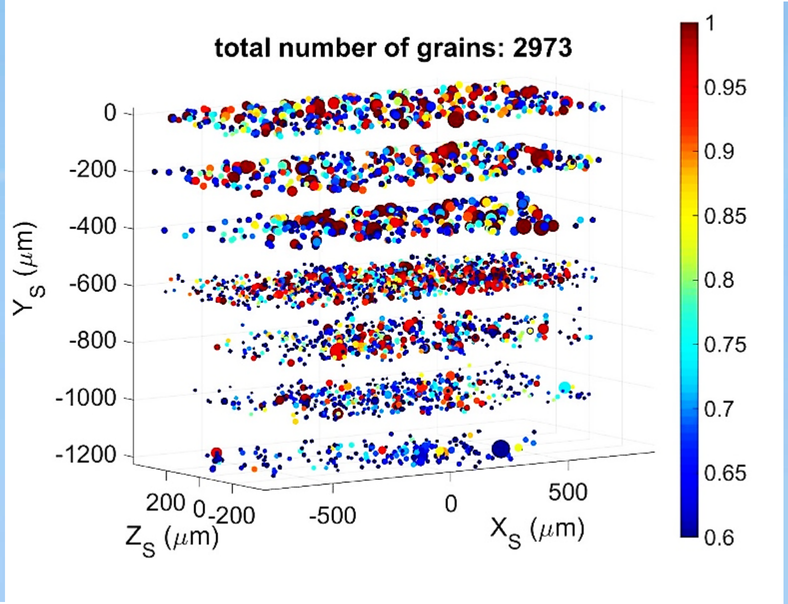

- **Comprehensive information**
  - **grain center of mass**
  - **grain volume**
  - **orientation**
  - **micro-strain**

Ref: Zhang X *et. al.*, *submitted to* ***Review of Scientific Instruments (2017)***

Modeling Effort

Materials science based logic for modeling general material degradation

Model → Based on the changes of stress / strain in materials using

Analytical modeling
Finite element analysis techniques
Neural network analysis

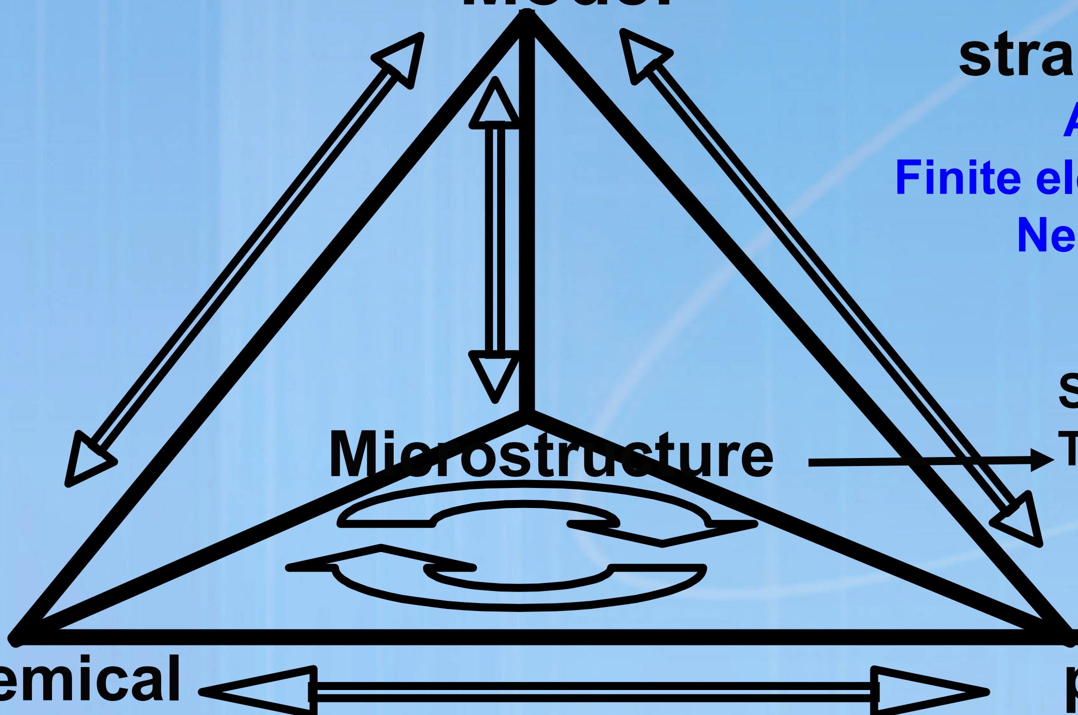

Microstructure → SEM – Topological Changes
TEM – Microstructural Changes

Chemical changes

Changes in the chemical composition using Atom Probe Tomography (APT)

Changes in the physical structure

On the Surface or Within the Structure

Mechanical properties
Hardness using Nano indentation
Structure using X-ray diffraction (XRD)

Example: Neural Network Modeling of Amorphous (Glassy) Steels

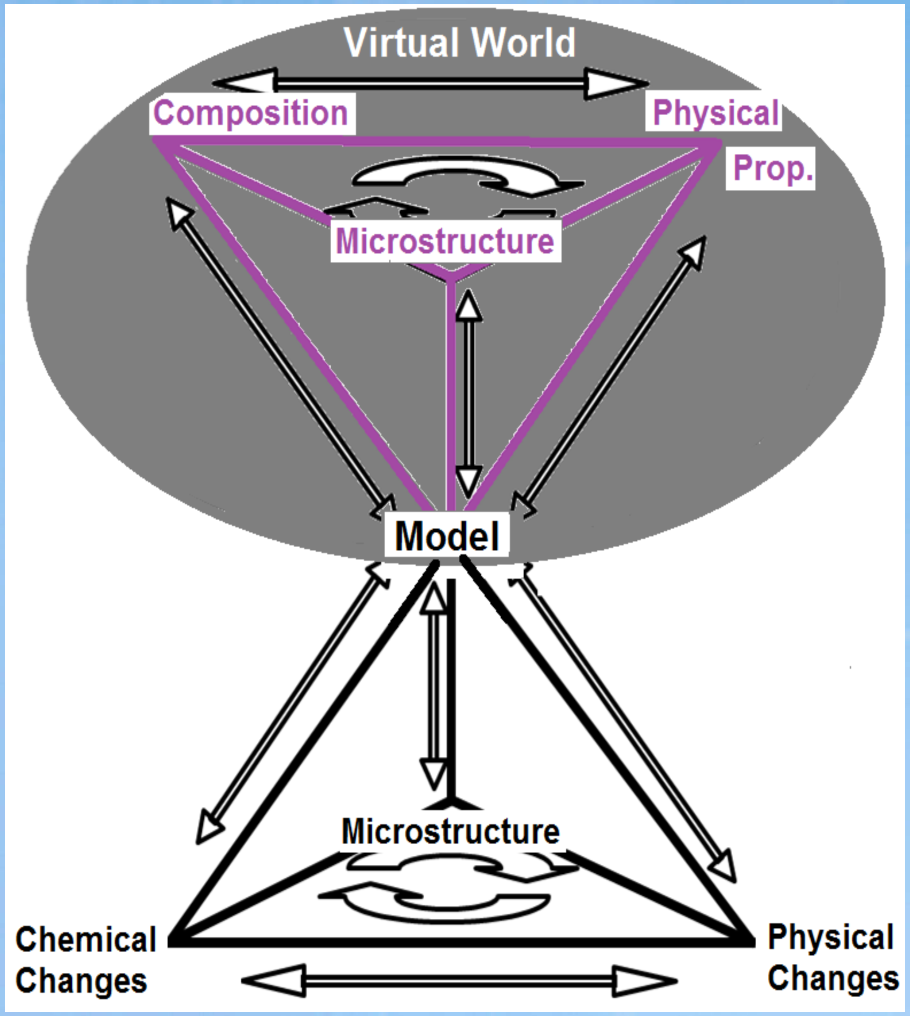

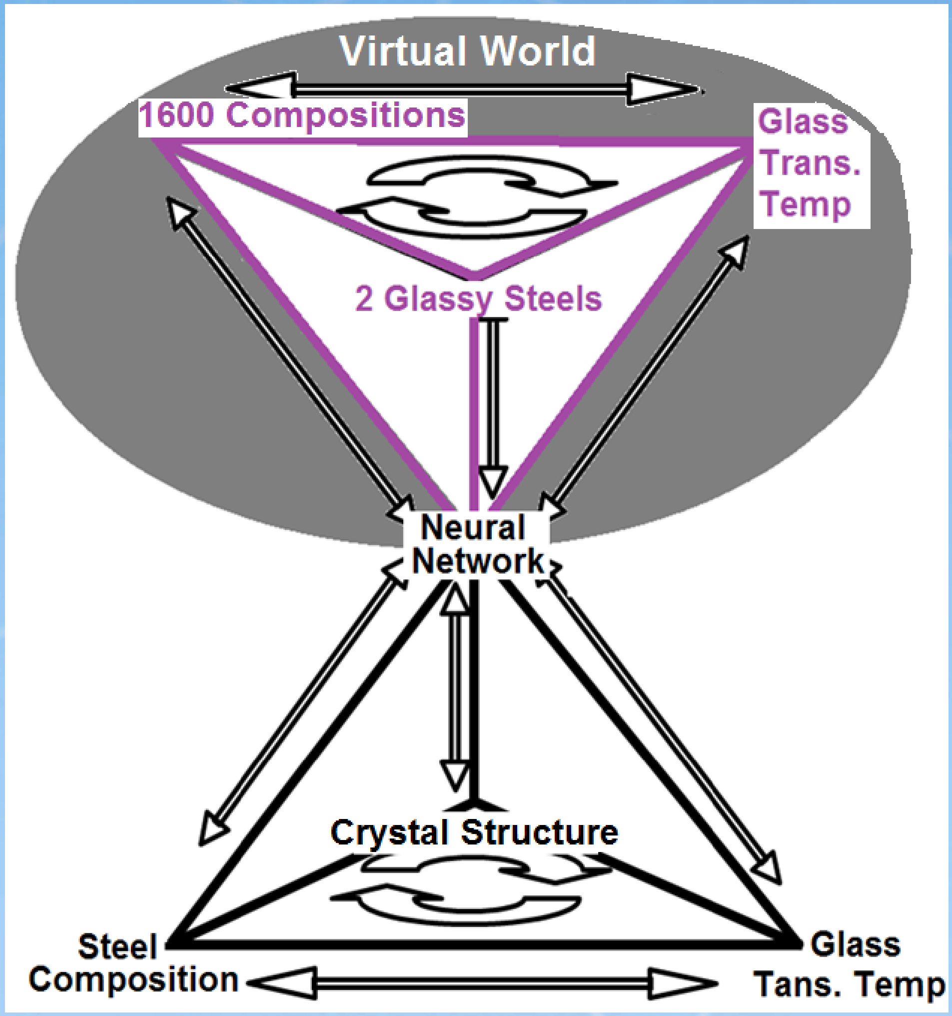

Ref: A. S. Rao, "Modeling of High Carbon, High Nickel Steel", NSWCCD-61-TR-2005/04, Jan. 2005.

Example: Analytical Modeling Based Life-Cycle Prediction

U.S.NRC
UNITED STATES NUCLEAR REGULATORY COMMISSION
Protecting People and the Environment

Treat Deformation Process → Only Precursor for the Nucleation of Defects → Defects → Introduce Various Stresses → Result → Material Failure

Deformation Problem → Translated into → Mechanics Problem

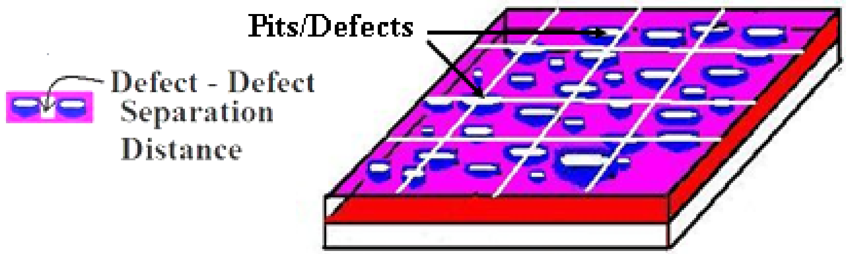

Plot {ln (1/Prob. of Survival)} versus ln{Dynamic stress (σ)}

Slope = R → "Rao Material Integrity Constant"

- R is High → Materials is Strong & Integrity High
- R is Low → Material Integrity is low

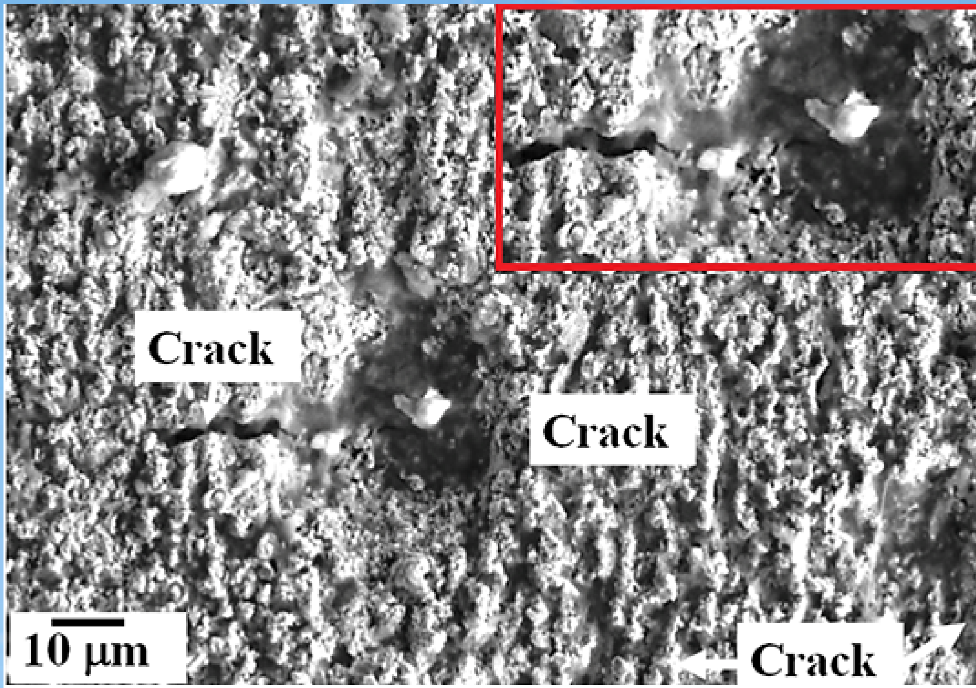

Duration of corrosion testing (days)	Average pit / craters / defects depth (µm)	Probability of failure of the NAB surface under the 45 ksi applied stress (%)	
		Upper boundary	Lower boundary
35	6.0 ± 1.5	82 ± 15	> 95 ± 5

Ref: Rao, A. S., *Trans. Of 21st SMIRT Conf., Nov. 2011.*

U.S.NRC
UNITED STATES NUCLEAR REGULATORY COMMISSION
Protecting People and the Environment

Transformation of Microstructure for Modeling

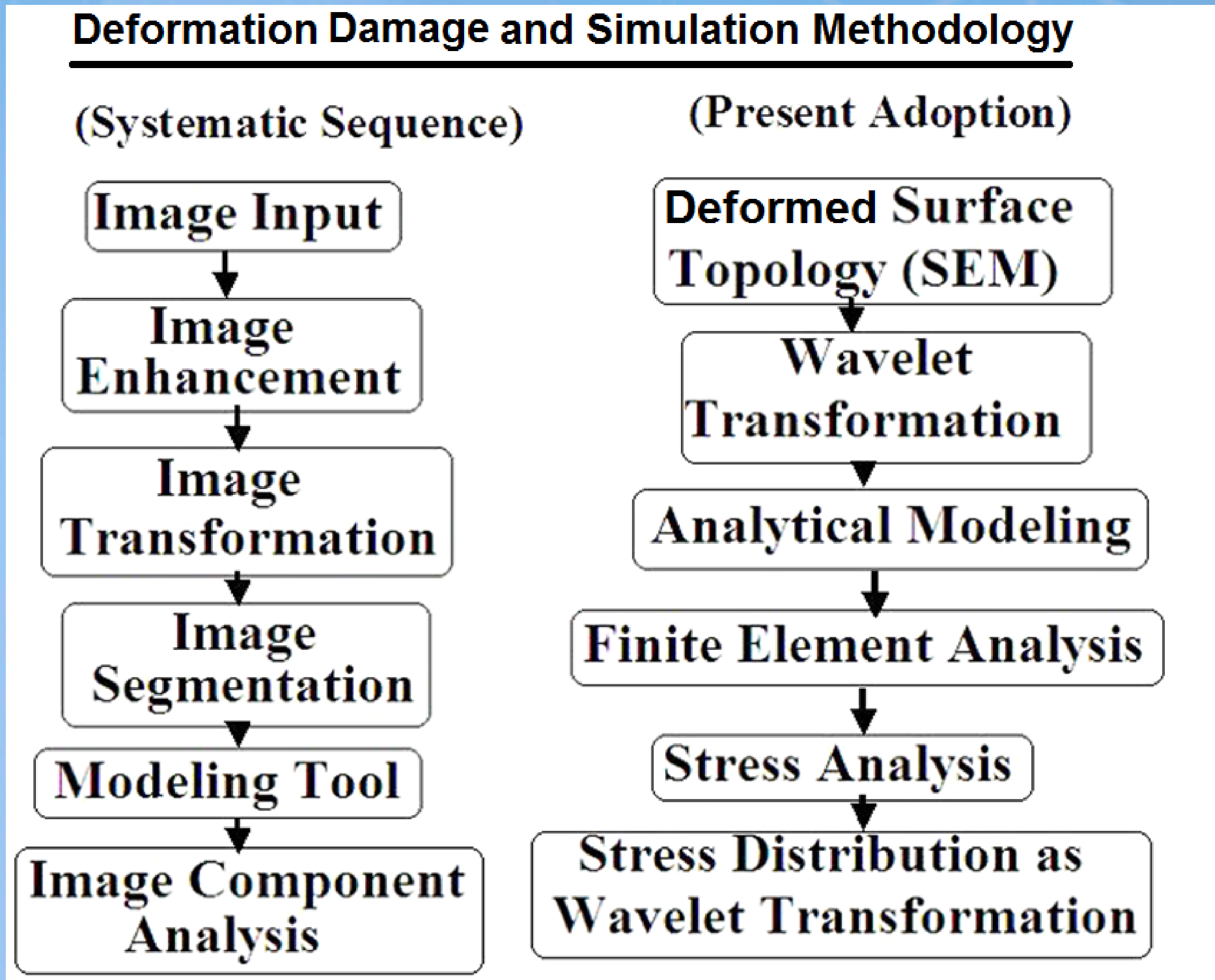

Example: FEA Modeling on Failure of Aluminum Alloy

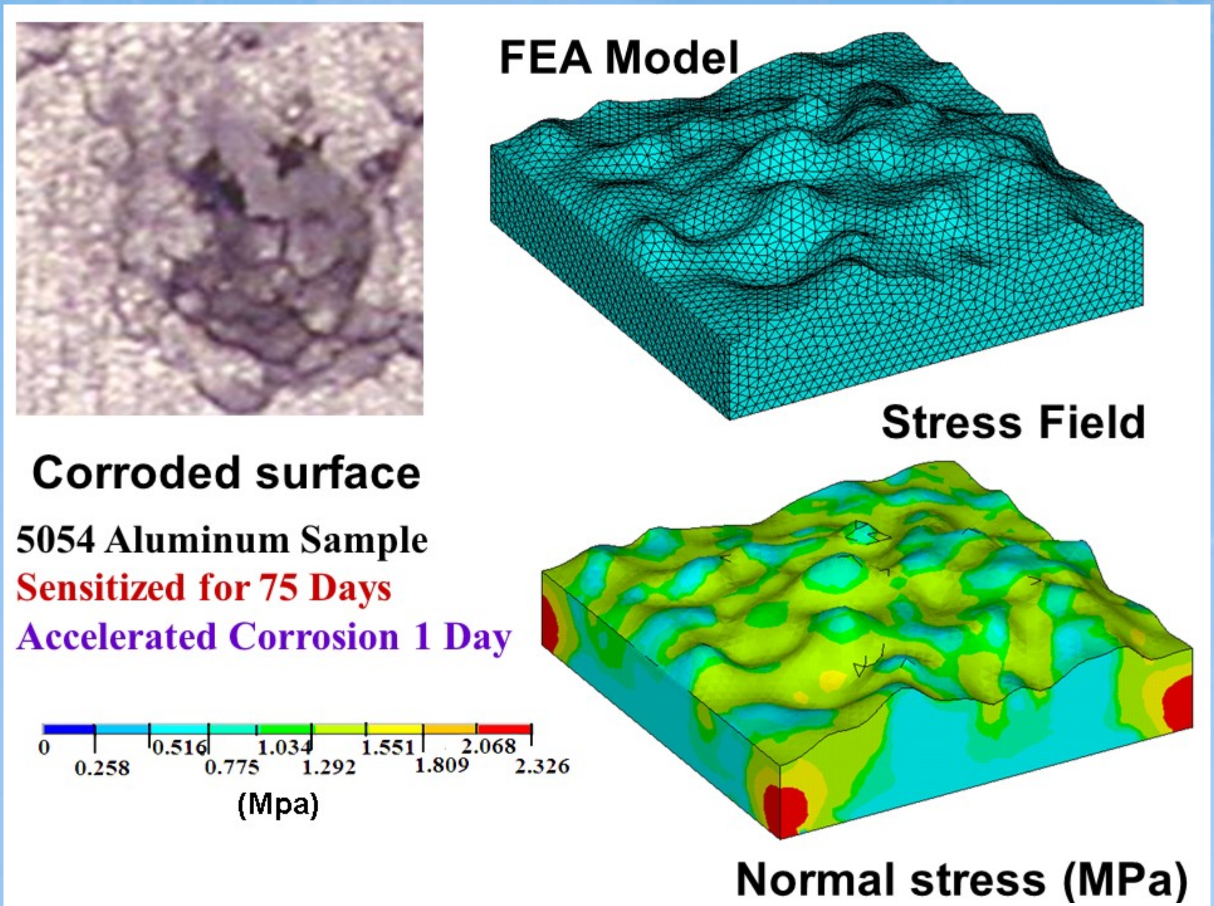

Ref: Rao *et. al., NSWCCD Report (2006)*

- From the stress field shown in the figure, the change in the normal stress was calculated.
- The change in the total stress including the contribution from shear stress was calculated.
- The total stress (von Mises stress) on the top layer was computationally isolated.
- This total stress on the top layer was plotted for analysis.

Projection of Crack Propagation Due to Stress in Aluminum Alloy

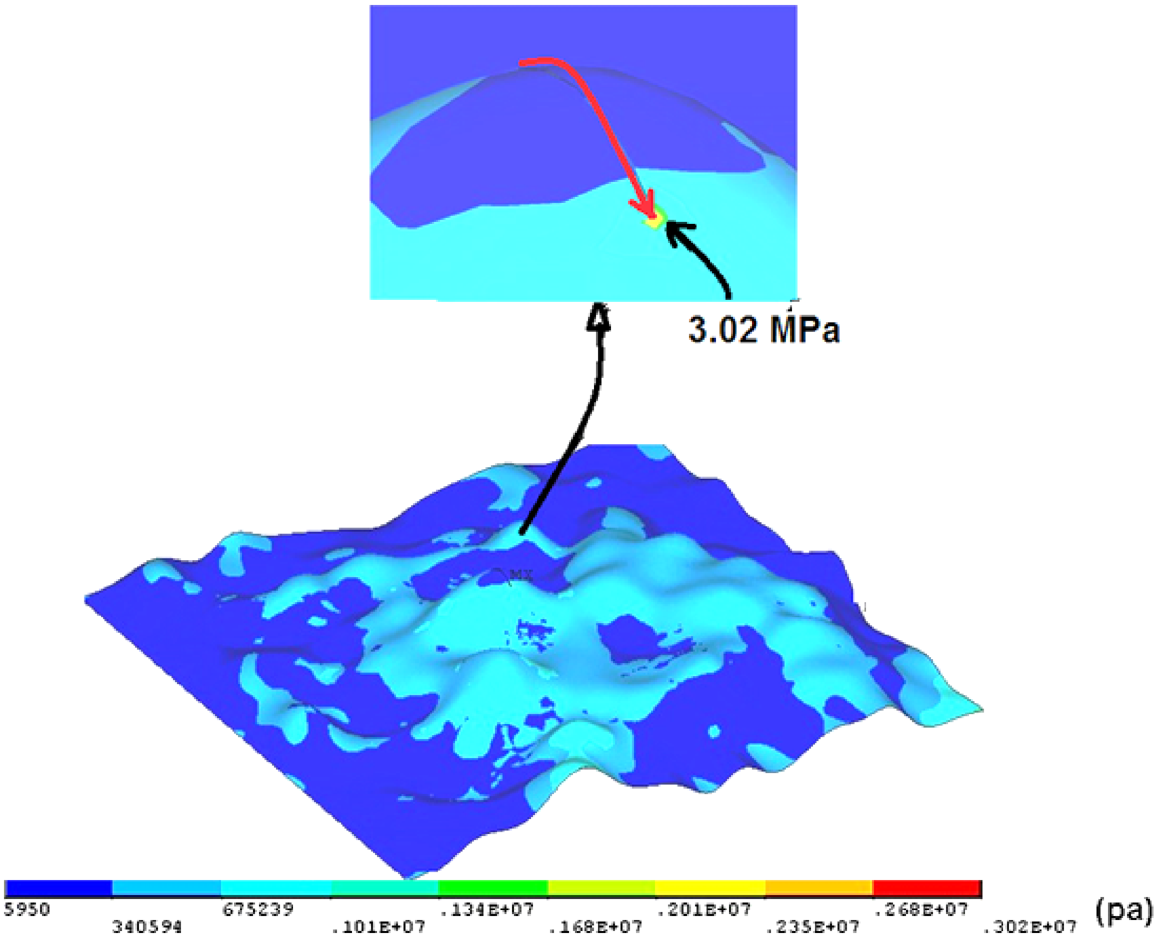

Von Mises Stress Field

Rao et.al., Journal of the Computational Mechanics, #365662, 10[2] 2009.

- The figure shows the total stress distribution of the top layer of the stressed aluminum alloy.
- The actual location where the stress exceeded the fracture stress of aluminum alloy (> 3.02 Mpa) was identified and located.
- Then the FEA algorithm will trace the shortest path the crack will follow in the event any additional stress was applied to the sample.

FEA Modeling

- High energy X-ray diffraction method provides information on lattice strain.
- TEM provides loop density and size. We can estimate the stress induced by these defects.
- SSRT and FT results provides information on fracture mode
- APT provides the distribution, size, and shape of the ferrite phase.
- Existing XFEM capabilities in ABAQUS will be used to model crack nucleation, growth and coalescence of the defects.
- The crack growth in a CT specimen will be simulated using ABAQUS.
- For the large plastic deformation, we will adopt local stress and strain failure criteria to assess the occurrence of the de-bonding of ferrite/austenite phase interface and the fracture of ferrite and austenitic matrix.

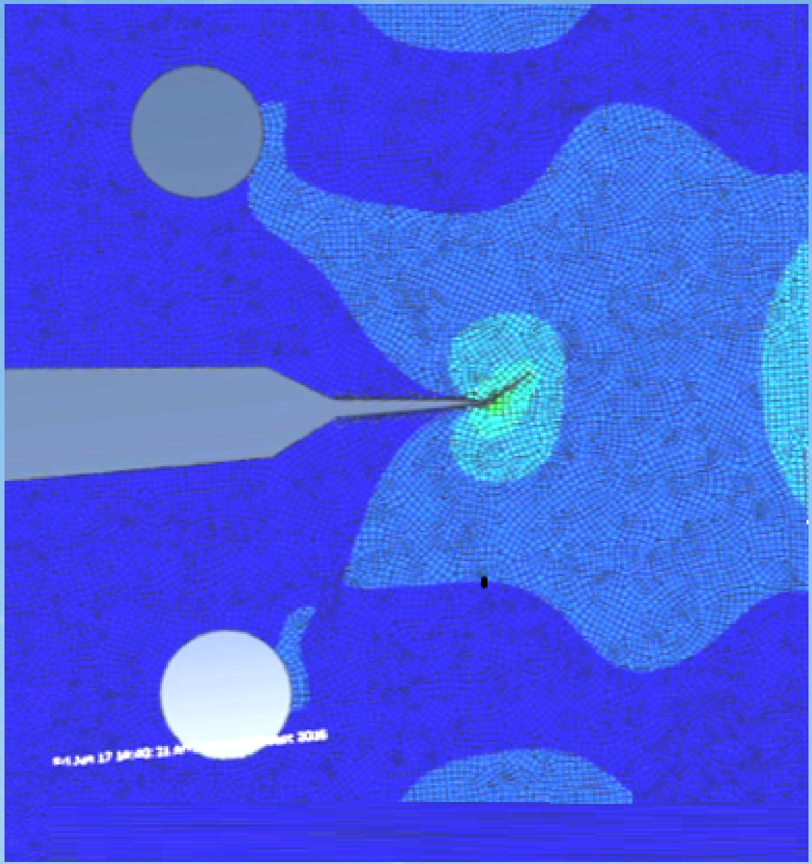

Example of the crack growth in a mono-phase material simulated using XFEM approach in ABAQUS.

Note: Modeling to start in FY 18 at the Univ. of Florida and Univ. of Georgia

Model Approach for Crack Initiation / Growth in Welds Under External Applied Stress

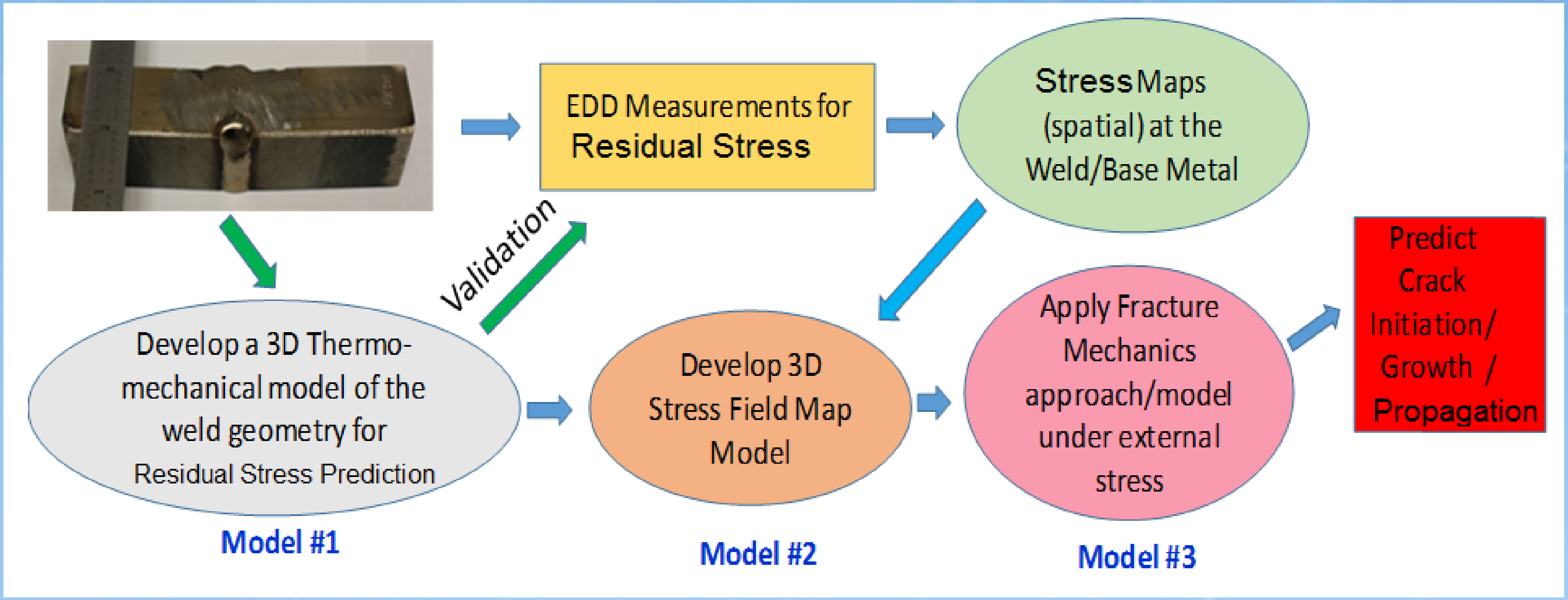

Note: Experimental testing of welds at ANL and Modeling effort to start in FY 18 at the Univ. of Georgia

U.S.NRC
UNITED STATES NUCLEAR REGULATORY COMMISSION
Protecting People and the Environment

Summary

- Radiation induced segregation (RIS) results in GB depletion of Cr, Mn, Mo & enrichment of Ni, Si, P, C, B. The segregation depends strongly on irradiation temperature, dose and dose rate.
- Atom probe tomography (APT) results suggests that neutron irradiation and thermal aging resulted in similar segregations of Cr and Fe (α/α' decomposition).
- Intergranular (IG) cracking is severe in the high-sulfur Type 304 SS and No IG cracking is observed in low-S 304 SS
- Neutron irradiation reduced fracture toughness in both unaged and aged CASS alloys.
- For CASS samples irradiated to 2.9 dpa, resistance in crack propagation is decreased.
- TEM microstructure of irradiated CASS suggests that dislocation loops are the main irradiation-induced microstructure in austenite and in ferrite a mixture of dislocation loops and G-phase precipitates are present.
- The hardness of δ- ferrite and γ-austenite can be measured more accurately using nano-indentation technique.

Summary cont.

- The hardness of γ-austenite phase of CASS is not affected by the thermal treatment, however, the hardness of δ- ferrite increases with thermal aging.
- While the hardness of γ-austenite phase of CASS is not affected by the low dose irradiation, the hardness tend to increase with neutron dose above 20 dpa. The hardness of δ- ferrite increases with neutron irradiation.
- High energy X-ray diffraction is a powerful and sensitive technique to observe subtle changes in internal microstructure of austenite or ferrite phase.
- Neutron irradiation of the 316 stainless steel changes the deformation mode from homogeneous to localized.
- Martensitic phase transformation plays an important role in the work-hardening mechanism.
- FEA modeling provides reasonably accurate prediction on the crack propagation in materials subjected to external stress.

Acknowledgement

I would like to thank the following for their help:

- Dr. Omesh Chopra (ANL- Gap analysis)
- Dr. Yiren Chen (ANL - Mechanical testing)
- Dr. Xuan Zhang (ANL- High energy XRD)
- Prof. Yong Yang (Univ. of Florida - APT)\
- Dr. Wei-Ying Chen, TEM characterization
- Dr. Amy Hull
- Dr. Pat Purtscher

U.S.NRC
UNITED STATES NUCLEAR REGULATORY COMMISSION
Protecting People and the Environment

References

- **Chen,Y. et al., NUREG/CR – 6965 (2008)**
- **Chen,Y. et al., NUREG/CR – 7128(2012)**
- **Chen,Y. et al., NUREG/CR – 7084(2015)**
- **Chen, Y. et al., Env. Deg. Conf., (2017)**
- **Chen et al., J. Nucl. Mater., 466, 560 (2015)**
- **Chopra, O. NUREG/CR – 7027(2010)**
- **Das, S. et al., J. Nucl. Mater., (1977)**
- **David, S.A., et al, Journal Of Metals, June, 2003**
- **Edwards, S. et al., 13th Intl. Conf. Env. Degrad., P0139, (2007)**
- **Li et al., J. Nucl. Mater, 466, 201 (2015)**
- **Mazey etal., J. Nucl. Mater., 64,145 (1977)**
- **Rao et. al.,** NSWCCD-TR **Report (2006)**
- **Rao, A., et al., J. of Computational Mechanics #365662, 10[2] (2009)**
- **Yong et.al., To be published in J. Nucl. Mater., (2017)**
- **Zhang X et. al.,** submitted to **Review of Scientific Instruments (2017)**

U.S.NRC
UNITED STATES NUCLEAR REGULATORY COMMISSION
Protecting People and the Environment

Acronyms

- APT Atom probe tomography
- BWR Boiling water reactor
- CASS Cast stainless steel
- CGR Crack growth rate
- CW Cold worked
- dpa Displacement per atom
- FEA Finite element analysis
- FT Fracture toughness
- GB Grain boundaries
- High-O High oxygen
- High-S High sulfur concentration
- HP High performance
- IG Intergranular
- Low-O Low oxygen concentration
- Low-S Low sulfur concentration
- LWR Light water reactor
- PWR Pressurized water reactor
- RIS Radiation induced segregation

Acronyms (cont.)

- RVI Reactor vessel internal
- RA Reduction in area of the cross-section of a sample
- SAXS Small angle x-ray scattering
- SA Solution annealed
- SEM Scanning electron microscope (microscopy)
- SS Stainless steel
- SSRT Slow strain rate test
- TEM Transmission electron microscope (microscopy)
- TG Transgranular
- WAXS Wide angle x-ray scattering
- XRD x-ray diffraction
- YS Yield stress